

Fabrication of three-dimensional (3-D) corneal transplantable model from silk  
fibroin/gelatin-based biomaterial



A Dissertation Submitted in Partial Fulfillment of the Requirements  
for the Degree of Doctor of Philosophy in Veterinary Biosciences

Department of Veterinary Anatomy

FACULTY OF VETERINARY SCIENCE

Chulalongkorn University

Academic Year 2020

Copyright of Chulalongkorn University

การสร้างตัวอย่างกระจกตา 3 มิติเพื่อการปลูกถ่าย จากวัสดุชีวภาพที่ สร้างจากไหม  
ไฟโบรอินและเจลาติน



วิทยานิพนธ์นี้เป็นส่วนหนึ่งของการศึกษาตามหลักสูตรปริญญาวิทยาศาสตรดุษฎีบัณฑิต  
สาขาวิชาชีวศาสตร์ทางสัตวแพทย์ ภาควิชากายวิภาคศาสตร์  
คณะสัตวแพทยศาสตร์ จุฬาลงกรณ์มหาวิทยาลัย  
ปีการศึกษา 2563  
ลิขสิทธิ์ของจุฬาลงกรณ์มหาวิทยาลัย



ชุตีรัตน์ ต่อสหัสกุล : การสร้างตัวอย่างกระจกตา 3 มิติเพื่อการปลูกถ่าย จากวัสดุชีวภาพที่สร้างจากไหมไฟโบรอินและเจลาติน. ( Fabrication of three-dimensional (3-D) corneal transplantable model from silk fibroin/gelatin-based biomaterial) อ.ที่ปรึกษาหลัก : ผศ. ดร.เจนภพ สว่างเมฆ, อ.ที่ปรึกษาร่วม : ผศ. ดร.จุฑามาศ รัตนวราภรณ์, ผศ. ดร.ศิริกานต์ ฐิตวัฒน์

ความผิดปกติของกระจกตาสุนัขเป็นสาเหตุสำคัญที่ทำให้สุนัขสูญเสียการมองเห็น หรือการมองเห็นลดลง ในขณะที่ความต้องการการปลูกถ่ายกระจกตามีความจำเป็นมากขึ้นเรื่อยๆ แต่วัสดุที่ใช้ในการปลูกถ่ายกระจกตาสุนัขทางคลินิกกลับมีไม่มากนัก ซึ่งในปัจจุบันมีเพียงแค่การใช้วัสดุปราศจากเซลล์ทางชีวภาพ และการใช้เนื้อเยื่อทดแทนจากตัวสัตว์เอง การศึกษานี้จึงมุ่งเน้นการผลิตวิศวกรรมเนื้อเยื่อกระจกตาในส่วนชั้นผิวของกระจกตาและชั้นสโตรมา ในส่วนของชั้นผิวกระจกตานั้นใช้สเต็มเซลล์ที่ผิวของกระจกตาร่วมกันกับแผ่นฟิล์มจากไหมไฟโบรอินและเจลาติน ส่วนของชั้นสโตรมาใช้สเต็มเซลล์จากกระจกชั้นสโตรมาและวัสดุโครงร่างจากไหมไฟโบรอินและเจลาตินเช่นกัน การศึกษานี้ได้มีการสกัดเซลล์ทั้ง 2 ชนิดโดยใช้เอนไซม์คอลลาจิเนส เมื่อนำเซลล์ทั้ง 2 ชนิดมาเลี้ยงร่วมกันกับแผ่นฟิล์ม และวัสดุโครงร่างพบว่าเซลล์สามารถยึดเกาะ เจริญเติบโต และรักษาความเป็นสเต็มเซลล์ของผิวกระจกตาได้ โดยบ่งชี้จากการแสดงออกของยีน *Abcg2* และ *P63* ซึ่งเป็นยีนที่จำเพาะต่อสเต็มเซลล์ชั้นผิวของกระจกตา และการย้อมติดแอนติบอดีของ *P63* สำหรับเซลล์ชั้นสโตรมาที่เลี้ยงในสภาวะที่กระตุ้นให้พัฒนาไปเป็นเซลล์ชนิดเคอราโตไซต์ยังพบว่า การนำเซลล์ไปเลี้ยงในวัสดุโครงร่างนั้น พบการแสดงออกของยีน *Lum*, *Aldh3a1* และ *Aqp1* ซึ่งเป็นยีนที่จำเพาะต่อเซลล์เคอราโตไซต์ และการย้อมแอนติบอดีของ *Aldh3a1* lumican และ collagen I ซึ่งบ่งชี้ถึงความสามารถในการสร้างคอลลาเจนและเมทริกซ์นอกเซลล์เช่นเดียวกับกระจกตาที่แท้จริง ผลจากการศึกษานี้สามารถนำไปใช้ป็นองค์ความรู้ในการพัฒนาวิศวกรรมเนื้อเยื่อกระจกตาของสุนัข เพื่อนำไปใช้สำหรับการปลูกถ่ายต่อไปในอนาคต

สาขาวิชา	ชีวศาสตร์ทางสัตวแพทย์	ลายมือชื่อนิสิต .....
ปีการศึกษา	2563	ลายมือชื่อ อ.ที่ปรึกษาหลัก .....
		ลายมือชื่อ อ.ที่ปรึกษาร่วม .....
		ลายมือชื่อ อ.ที่ปรึกษาร่วม .....

# # 5975505231 : MAJOR VETERINARY BIOSCIENCES

KEYWORD: Canine limbal epithelial stem cells (cLESCs) Canine corneal stromal stem cell (cSSCs) Silk fibroin Gelatin Tissue engineering

Chutirat Torsahakul : Fabrication of three-dimensional (3-D) corneal transplantable model from silk fibroin/gelatin-based biomaterial. Advisor: Asst. Prof. Chenphop Sawangmake, DVM.MSc.PhD Co-advisor: Asst. Prof. JUTHAMAS RATANAVARAPORN, Ph.D.,Asst. Prof. SIRAKARNT DHITAVAT, Ph.D.

Canine corneal blindness is a common cause of vision loss and visual impairment worldwide. While the demand of canine corneal graft is continuously elevated, the clinical useable grafts are limited to acellular biomaterials and allograft. This study aimed to generate the tissue-engineered canine cornea in the part of corneal epithelium and underlying stroma based on cLESCs (canine limbal epithelial stem cells) seeded silk fibroin and gelatin (SF/G) film and cSSCs (canine corneal stromal stem cells) seeded SF/G scaffold respectively. Both cell types were successfully isolated by collagenase I. SF/G films and scaffolds served as the prospective substrates for cLESCs and cSSCs by promoting cell adhesion, cell viability and cell proliferation. Furthermore, gene expression levels were compared among cells seeded tissue culture plate (TCP) and cells seeded their own scaffolds. Here, the results revealed the upregulation of *P63* and *Abcg2* of cLESCs as well as *Kera*, *Lum*, *Aldh3a1* and *Aqp1* which are the marker of cells differentiated into keratocytes and extracellular matrix production like a native cornea. Moreover, immunohistochemistry was illustrated the positive staining of P63, lumican, Aldh3a1 and collagen I. The results manifested the feasible platform to construct tissue-engineered canine cornea as the functional transplantable corneal grafts and provided the profitable acknowledgement in the area of canine corneal stem cells to develop stem cell-based therapy in the future.

Field of Study: Veterinary Biosciences

Academic Year: 2020

Student's Signature .....

Advisor's Signature .....

Co-advisor's Signature .....

Co-advisor's Signature .....

## ACKNOWLEDGEMENTS

Firstly, I would like to express my gratitude for the 100th Anniversary Chulalongkorn University Fund for Doctoral Scholarship, the 100th Anniversary Chulalongkorn University Fund, Chulalongkorn University for financial support.

I would like to acknowledge the chairman of thesis committee, Assoc. Prof. Dr. Meena Sarikaputi, members of thesis committee, Asst. Prof. Dr. Naline Tuntivanich, Prof. Dr. Thanaphum Osathanon, and Assoc. Prof. Dr. Sirikul Manochantr, for kindly providing useful comments to the study.

For the success on the study and thesis project, I would like to express my deepest gratitude to my thesis principal advisor and instructor, Asst. Prof. Dr. Chenphop Sawangmake (DVM, MSc, PhD), and my thesis principal co-advisor, Asst. Prof. Dr. Sirakarnt Dhitavat and Asst. Prof. Dr. Juthamas Ratanavaraporn for supporting and taking care of me until reaching the destination.

For other kind supports, I would like to express my appreciation to Professor Dr. Kaywalee Chatdarong (DVM, PhD), for supporting on qPCR analysis; Assoc.Prof.Dr. Sayamon Srisuwattanasagul for providing knowledge of cell staining and antibodies; Assoc. Prof. Dr. Nipan Israsena, M.D., for providing knowledge of cell culture and feeder cells; Professor Prasit Pavasant (DDS, PhD); Professor Thanaphum Osathanon (DDS, PhD), Center of Excellence for Regenerative Dentistry, Faculty of Dentistry, Chulalongkorn University, for supporting and helping on research work and the Veterinary Stem Cell and Bioengineering Innovation Center (VSCBIC) (<http://www.cuvsbic.com/>), Faculty of Veterinary Science, Chulalongkorn University, for providing research facility support and Small Animal Hospital Faculty of Veterinary Science; Rak na chan veterinary hospital; Phyathai 7 veterinary hospital; Pranee veterinarian Eyes Animal Disease Center for providing eye samples.

For biggest supporters, I deeply thank my beloved family, my relatives and my colleague for big supporting, encouraging, and giving all their love to me all along.

Chutirat Torsahakul

## TABLE OF CONTENTS

	Page
ABSTRACT (THAI).....	iii
ABSTRACT (ENGLISH).....	iv
ACKNOWLEDGEMENTS.....	v
TABLE OF CONTENTS.....	vi
LIST OF TABLES.....	ix
LIST OF FIGURES.....	x
CHAPTER I.....	1
INTRODUCTION.....	1
Important and rational.....	1
Objectives.....	4
Keywords (English).....	4
Keywords (Thai).....	4
Hypothesis.....	4
CHAPTER II.....	5
LITERATURE REVIEW.....	5
Part 1 cornea.....	5
1.2 Structure and Properties of the Corneal Epithelium.....	6
1.3 Structure and Properties of the Corneal Stroma.....	9
Part 2 Tissue engineering.....	11
2.1 Definition of Tissue Engineering.....	11
2.2 Corneal cell Sources for Tissue Engineering.....	12

2.3 Tissue Engineering Scaffolds .....	13
2.3.1. Silk fibroin (SF) .....	14
2.3.2 Gelatin.....	16
2.2.3 Silk fibroin/gelatin (SF/G) blended scaffold .....	17
Conceptual framework.....	18
Experimental plan .....	19
CHAPTER III .....	20
Materials and methods .....	20
1. Preparation of silk fibroin solution (SF).....	20
2. Preparation of gelatin (G).....	20
3. Preparation of Silk fibroin/gelatin (SF/G) films .....	20
4. Preparation of Silk fibroin/gelatin (SF/G) scaffolds.....	21
5. Material morphological and structural characterization .....	21
6. Swelling test .....	22
7. <i>In Vitro</i> enzymatic degradation .....	22
8. Uniaxial tensile test .....	22
9. Canine limbal corneal epithelial cell (cLECs) isolation and culture .....	23
11. Canine corneal stromal stem cells (cSSCs) isolation and culture .....	24
12. Keratocyte differentiation .....	25
13. Quantitative reverse transcription PCR (RT-qPCR) .....	25
Mesenchymal stemness marker.....	26
14. Cell proliferation assay .....	28
15. Cell viability assay and distribution .....	29
16. Bio-fabricated cornea formation.....	29



17. Histology, immunocytochemistry and immunohistochemistry.....	31
18. Statistical analysis .....	32
CHAPTER III .....	33
RESULTS and DISCUSSION .....	33
Results.....	33
cLESCs and cCSSCs isolation and characterization .....	33
SF/G film and scaffold fabrication and characterization.....	35
Physical properties of SF/G film and Scaffold.....	37
Implemented SF/G films and scaffolds provided favorable biocompatibility...	40
Bio-fabricated corneal equivalents .....	45
Discussion .....	48
CHAPTER 5.....	56
CONCLUSION .....	56
REFERENCES .....	57
VITA.....	75

## LIST OF TABLES

	Page
Table 1: Primer sequences.....	26
Table 2: Elastic Modulus, UTS, and % elongation at break .....	35



## LIST OF FIGURES

	<b>Page</b>
Figure 1: cross-sectional of the cornea (Chen et al., 2018).....	6
Figure 2: Parallel orientation of collagen fibrils in lamella collagen stroma, transverse section (Robert et al., 2001) (a), and perpendicular alignment of each collagen lamellae (Meek and Fullwood, 2001) (b).....	11
Figure 3: A common methodology of tissue engineering (Kim and Mooney, 1998) ...	12
Figure 4: cLESCs and cSSCs characterization.....	34
Figure 5: SF/G film and scaffold characterization. ....	37
Figure 6: cLESCs seeded SF/G film and cSSCs seeded scaffold.....	38
Figure 7: mRNA expression of cLESCs seeded SF/G film and cSSCs seeded scaffold. .....	40
Figure 8: Bio-fabricated cornea.....	43
Figure 9: Morphology and immunocytochemical profiles. ....	45
Figure 10: Immunofluorescent staining of Collagen I.....	47

## CHAPTER I

### INTRODUCTION

#### **Important and rational**

The cornea is a transparent soft tissue located at the outermost of the eye. According to its transparency, the whole light ray is modulated in term of refraction and transmission of the incoming light focusing onto the lens to create clear vision. It also protects the eyes from many types of hazard such as germs, dust and chemical or mechanical substances due to its integrity. In human and animal, corneas consist of 5 recognized layers including 3 cellular layers (epithelium, stroma and endothelium) and 2 acellular layers (Bowman's layer and Descemet's membrane) (DelMonte and Kim, 2011). However, Bowman's membrane is not found in carnivores substituted by special stroma condensation (Merindano et al., 2003). All layers play an important role to maintain corneal strength, smoothness and clarity as a glass.

Corneal blindness is the third common causes of vision loss and vision impairment inferior to cataract and glaucoma (Petrick, 1996), reported approximately 4.9 million cases for bilateral corneal blindness worldwide (Oliva et al., 2012). Trauma resulting in corneal ulcer, keratitis and trachoma were found as the major causes of corneal blindness in human (Whitcher et al., 2001) and the prevalence of canine ulcerative disease had been up to 0.80% in England (834 from 104,233 dogs) (O'Neill et al., 2017). Corneal grafts have become the most common treatment for tissue transplantation in human eyes, 60,000 to 80,000 performed annually in the US (Eye Bank Association of America, 2015) as well as animal eyes. With regard to canine, the corneal graft has been widely used in clinical applications and preclinical trials including conjunctival autograft, nictitating membrane flap (Maggs et al., 2012), human amniotic membrane (Barros et al., 1998; Barros et al., 2005; Vongsakul et al., 2009), equine amniotic membrane (Arcelli et al., 2009; Ollivier, 2008), canine amniotic membrane (Kalpravidh et al., 2009) and porcine urinary bladder submucosa (ACell VetTM) (Bertoldi, 2016). However, some critical disadvantages of corneal graft transplantations have been

found such as disease transmission, contamination, limited tissue shelf life, specific storage condition ( $-86\text{ }^{\circ}\text{C}$ ) and graft rejection associated with biological variability (Maharajan et al., 2007; Utheim et al., 2015).

Recently, to rectify those problems, the alternative biosynthetic corneal substitutes are synthesized based on the knowledge of cell culture and tissue engineering. Corneal stem cell-based therapy possesses the promising cell source in tissue engineering such as limbal epithelial stem cells (LESCs) and corneal stromal stem cells (CSSCs) (Ghezzi et al., 2015). LESCs have a potential to generate corneal epithelial cells which are the terminal differentiated cells as well as CSSCs have been progressed in respect of stem cell properties (clonal growth *in vitro*, extended lifespan, and the ability of differentiation in particular keratocytes) (Du et al., 2005). Hence, LESCs and CSSCs are pointed to be investigated in term of isolation technique, expansion, characterization, culture and differentiation in a tissue-engineered scaffold *in vitro* to approach bona fide cornea.

Various materials have been used to fabricate three-dimensional (3-D) biocompatible scaffolds which are able to imitate natural extracellular matrix (ECM) and support cell attachment and growth such as silk protein (SF). Silk composed of 2 main proteins which are water-soluble sericin and water-insoluble fibroin. The advantages of SF are demonstrated ex. good tensile strength, easy to be fabricated into various forms, high availability, degradability, transparency and non-immunogenic response (Kundu et al., 2012; Omenetto and Kaplan, 2010). Consequently, SF has become a favorable replacement for ocular tissue. There are several supported reports in regard to corneal epithelial scaffold (Bray et al., 2011; Gosselin et al., 2018; Hazra et al., 2016; Lawrence et al., 2009; Liu et al., 2012), corneal stromal scaffold (Hazra et al., 2016; Lawrence et al., 2009; Wu et al., 2014b) as well as co-culturing system *in vivo* and *in vitro* (Bray et al., 2012; Gosselin et al., 2018).

Nonetheless, some disadvantages have been found, SF has slow degradation rate and yellow tinted color which is raised to be an important concern in optical clarity and eye comfort after transplantation (Numata et al., 2010; Rockwood et al., 2011; Wang et al., 2008). Interestingly, to increase SF degradation rate, diminishing the formation of beta-amyloid structures, incorporation with other rapid-degrading materials has been revealed to accelerate degradation rate, such as gelatin (Jin et al., 2005; Numata et al., 2010; Wang et al., 2008; Yang et al., 2012). Gelatin is derived from partial hydrolysis of collagen and indicated superb biocompatibility and biodegradability. Regarding cornea bioengineering, gelatin has been used as an endothelial cell sheet grafts *in vivo* with satisfying outcomes (Lai et al., 2007; Niu et al., 2014).

This study aimed to investigate and optimize the silk film and scaffold modified with gelatin in appropriate proportion and formulation for culturing of canine limbal epithelial stem cells (cLESCs) and canine corneal stromal stem cells (cSSCs) to fabricate 3-D synthetic corneal tissue. The outcome of this study was a promising corneal graft for treating canine corneal defect and maintaining corneal transparency for a long period of time in clinical application. In addition, isolation techniques of cLESCs and cSSCs was replenished the knowledge of cell culture in veterinary medical profession and applied to use in further experiments.

## Objectives

1. To establish the effective isolation, culture and differentiation protocols of canine limbal epithelial stem cells (cLESCs) and canine corneal stromal stem cells (cCSSCs) for 3-D corneal construction.
2. To fabricate the appropriate scaffold for supporting cell proliferation, viability, distribution and persistence of canine limbal epithelial stem cells (cLESCs) as well as encouragement of keratocyte differentiation.
3. To synthesize 3-D tissue-engineered canine corneal characterized by morphology, cell distribution, collagen alignment and extracellular matrix production aiming to use as a transplantable corneal substitute.

## Keywords (English)

Canine limbal epithelial stem cells (cLESCs), Canine corneal stromal stem cell (cCSSCs), Silk fibroin, Gelatin, Tissue engineering

## Keywords (Thai)

เซลล์ต้นกำเนิดผิวกระจกตาของสุนัข เซลล์ต้นกำเนิดกระจกตาชั้นสโตรมาของสุนัข ไหมไฟโบรอิน เจลาติน วิศวกรรมเนื้อเยื่อ

## Hypothesis

Canine limbal epithelial stem cells (cLESCs) and canine corneal stromal stem cells (cCSSCs) have a capability to adhere, grow and differentiate within SF/G films and SF/G scaffolds in the optimized condition for construction of the tissue-engineered canine cornea mimicking native corneal tissue.

## CHAPTER II

### LITERATURE REVIEW

#### Literature review

#### Part 1 cornea

##### 1.1. Structure, function and componence of cornea

The cornea is the transparent outermost layer of the eye and the thickness of cornea is around 500-600 micrometers in humans and animals (Gilger et al., 1991; Liu et al., 1999). Cornea is non-vascular, elastic, clear and comprised of 5 distinct layers including 3 cellular layers (epithelium, stroma and endothelium) and 2 acellular layers (Bowman's layer and Descemet's membrane) (DelMonte and Kim, 2011). From outer to inner, corneal epithelium is an outermost part of cornea consisted of stratified squamous epithelial cells particularly lying on basement membrane. The function of epithelium is for preventing physical agents such as dust and germs out of the eyes and also permeable to promote nutrient and oxygen transportation pass through the inner layer of cornea (Liu et al., 1999). Basement membrane is located beneath basal epithelium cells and composed of various extracellular molecules including collagens, laminins, heparan sulfate proteoglycans, and nidogens. The function of basement membrane is to anchor epithelial cell with stroma in the absence of Bowman's layer species and associated with cytokines penetration in homeostasis and wound healing process (Torricelli et al., 2013). Beyond basement membrane, Bowman's layer which is fibrous collagen meshwork has been found in almost all primates and some herbivores but absent in all carnivores (Merindano et al., 2003). Followed by corneal stroma, the bulk of this tissue, 90% thickness of cornea, is comprised of regularly arranged collagen fibrils and sparse diffusion of keratocytes resulting in corneal transparency. Descemet's membrane, underneath corneal stroma, provides the lower barrier to protect infectious agents down below as well as supports the last single layer called endothelium. This layer is accountable for fluid balance within the cornea by compensating pump from overhydration and edematous condition. (Cursiefen et



al., 2003). Normally, all corneal layers would necessitate to be transparent with low light scattering and avascularity. Corneal transparency is caused by the homogeneity of the refractive index of all its constituent cells (Dohlman, 1971). Consequently, the alterations of one or more of corneal layers affect to increase in corneal light scattering associated with corneal opacity.

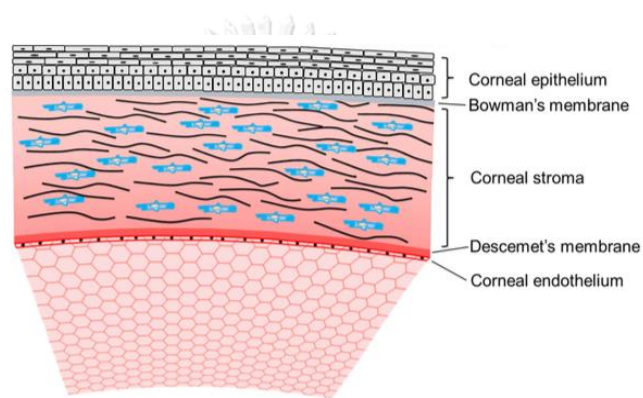


Figure 1: cross-sectional of the cornea (Chen et al., 2018)

## 1.2 Structure and Properties of the Corneal Epithelium

Epithelium is the outermost layer of cornea for protecting the eyes. Thickness of corneal epithelium around 40–50  $\mu\text{m}$  in human (DelMonte and Kim, 2011) and 80  $\mu\text{m}$  in canine (Helper, 1989). It comprises of 2-3 flat layers with glycocalyx-covered microvilli for tear film stabilization beneath 4-6 layers of nonkeratinized squamous epithelial cells (Wiley et al., 1991). Limbal epithelial stem cells (LESCs) are the precursor of corneal epithelium located at corneoscleral junction (Osei-Bempong et al., 2013) and underlying sclera, known as the palisades of Vogt (Osei-Bempong et al., 2013). The palisades of Vogt are characterized by infoldings to extend their surface area which is permeated with the vascular plexus for providing the nutrition from the

aqueous humour and the tear film (Huang et al., 2015). The basal epithelial cells are anchored to the basal lamina by hemi-desmosomes, whilst desmosomes hold cells together. Anyways, corneal epithelium provides a number of benefits to the cornea including being a barrier from physical substances, light refraction by acting together with tear and its smooth surface and transferring water and soluble substance into or out of lower layer. (Ghezzi et al., 2015).

In relation to limbal epithelial stem cells (LESCs), they are cuboidal in shape, small volume, high nucleus to cytoplasm ration compared to the basal cells of the central and peripheral cornea and higher proliferation ability associated with clonal analyzation (Chen et al., 2004; Pellegrini et al., 1999; Schlötzer-Schrehardt and Kruse, 2005). Underneath these structures, stromal crypt structures are corelative to the putative stem cell niches to facilitate the crosstalk between limbal basal cells with the CSSCs (corneal stromal stem cells), vessel network, extracellular matrix, and other cell types (Dziasko et al., 2014; Dziasko and Daniels, 2016). Moreover, melanocytes have been found closely adjacent to LESCs for preserving stemness and produced melanin to protect those cells from UV damage (Cotsarelis et al., 1989; Dziasko et al., 2015).

Particularly, the function of limbal epithelial stem cells (LESCs) is to maintain corneal epithelial cell homeostasis by dividing asymmetrically to stem cells and transient amplifying cells which migrate to basal center cornea and rise up to be superficial corneal epithelial cells respectively, and finally substitute the losing cell for every 7-10 days (Dua and Azuara-Blanco, 2000; Lavker and Sun, 2000; Liu et al., 1999). Limbal epithelial stem cells (LESCs) themselves are mitotically inactive and have a slow cycle which is illustrated by the maintaining of the marker trituerated thymidine ([<sup>3</sup>H]dT) for long chasing periods (Barbaro et al., 2007; Cotsarelis et al., 1989), whereas transient amplifying cells display high proliferative potential. On the ground of mitotic cells renewal capacity, LESCs play an important role for wound healing process by migration and cell spreading of the healthy cells toward the corneal defect by nonmitotic wound healing following by tissue reconstruction from mitotic cells which

are then arisen (Ljubimov and Saghizadeh, 2015). There is also reported to be angiogenic balance of LESC's anticipated in avascularity, thereby in case of limbal epithelial stem cells deficiency (LSCD), the balance shifts to pro-angiogenic condition resulting in corneal neovascularization (Lim et al., 2009).

Address to limbal stem cell marker, nowadays it remains unknown. There are several reports pursuing the relation of  $\alpha$  isoform of  $\nabla$ Np63 (N-terminally truncated transcripts generated by the p63 gene) and limbal stem cells in human and canine. Consequently, the result indicated significantly positive relation (Di Iorio et al., 2005; Nam et al., 2015). Besides, ABCG2 (Dziasko et al., 2015), cytokeratin15 (Meyer-Blazejewska et al., 2010), cytokeratin 14 (Nieto-Miguel et al., 2011), frizzled 7 (Mei et al., 2014), cytokeratin 7 (Mikhailova et al., 2015), and lately ABCB5 (Ksander et al., 2014) have been determined as putative LESC's stem cell markers.

The LESC's have been widely successful in isolation, culture and using as a corneal epithelium graft in human limbal stem cell deficiency (LSCD) (Tan et al., 1996). There are mentioned to be several therapeutic strategies to undergo ocular surface reconstruction (OSR) in case of LSCD including amniotic membrane transplantation (AMT) (Tseng et al., 1998), conjunctival limbal grafting (Keivyon and Tseng, 1989), allograft limbal stem cell transplantation (Daya et al., 2005), simple limbal epithelial transplantation (SLET) (Sangwan et al., 2012), and cultivated limbal epithelial transplantation (CLET) (Cheng et al., 2017). Recently, stem cell-based therapy and tissue engineering have become the effective technique for stem cell plasticity based on the principle of *in vitro* cells expanding on the substrate for ocular surface reconstruction (OSR) (Dong et al., 2018). In canine, LESC's have been addressed in the clinical improvement of allogenic limbal stem cell in subconjunctival use (Kovšca Janjatović et al., 2015), sclerocorneal limbal stem cell autograft transplantation in experiment (Brunelli et al., 2007) and as in corneal epithelial cell sheets cultivations (Nam et al., 2015).

### 1.3 Structure and Properties of the Corneal Stroma

Corneal stroma is the thickest layer, around 80-85% of corneal, 500  $\mu\text{m}$  thickness, and provides many vital biochemical properties such as transparency, tensile strength and stability. It comprises of heterogenous orthogonal collagen fibrils alignment including predominant collagen type I, collagen type III, collagen type V and collagen type VI (Marshall et al., 1991), proteoglycan and keratocytes which are sparsely dispersed in the whole collagen fibrils (Chen et al., 2015). The collagen fibrils are regularly arranged in diameter (250–340 nm diameter) and spaced responsible for flat lamella sheet forming. There are 250-300 distinct collagen lamellae in stroma which are aligned in perpendicular orientation especially in posterior stroma (Meek and Fullwood, 2001; Meek and Boote, 2004). Moreover, extracellular matrix (ECM) is also an important substance including a number of proteoglycans such as keratocan, lumican and biglycan as well as glycosaminoglycans including predominant keratan sulfate, chondroitin sulfate and dermatan sulfate. Those ECM molecules are associated with spacing and collagen fibril organization related to corneal transparency. There is a supporting report verified the significance of proteoglycans described by lumican knock-out causing corneal opacity (Chakravarti et al., 2000).

Revolving about keratocytes, corneal fibroblasts are mesenchymal cells derived from neural crest. They sparsely diffuse between 9-17% of tissue cellular volume and approximately 23,000 cells/mm<sup>3</sup> (Nickerson, 2015). They play an important role to facilitate lamellar organization and corneal stromal extracellular matrix by collagen and proteoglycan production resulting in corneal transparency. Keratocytes are transparent themselves by their crystalline protein such as aldehyde dehydrogenase type III. Moreover, keratocytes are essential for healing process by differentiation into fibroblast or myofibroblast which is producing more ECM components (Jester and Ho-Chang, 2003). Nevertheless, in severe injury, the expression of ECM disorganization might be occurred resulting in corneal opacity, so called corneal scar (Funderburgh et al., 2003). *In vitro*, keratocytes are hardly persisted in their gene

expression, morphology, and ability to organize corneal-like ECM after high passage number even in serum or serum free media. However, in the condition of a specific pattern of topographical scaffold, they can retrieve the capability to secrete typical organized ECM of corneal stroma (Karamichos et al., 2014).

Recently, discovering of keratocyte progenitor cells, human corneal stromal stem cells (hCSCs) have been progressed in respect of stem cell properties (clonal growth *in vitro*, extended lifespan, and the ability of differentiation in particular keratocytes), isolation and culturing procedures (Du et al., 2005). CSCs, neural crest-derived MSC, locate at the limbal stroma proximity to the limbal epithelial basement membrane (Funderburgh et al., 2016). Interestingly, hCSCs, *in vitro* and *in vivo*, have an ability to secrete multilayered lamellae with orthogonally oriented collagen lamellae resulting in corneal transparency, mimicking human corneal stromal tissue (Wu et al., 2014a) and modulating preexisting scars by corneal remodeling (Demirayak et al., 2016; Mittal et al., 2016; Tighe and Williams). For corneal healing, there are presented to be several paracrine effects related to corneal healing process including differentiated growth factors, migration of keratocyte, keratocyte apoptosis inhibitor and up-regulation of ECM of keratocyte genes (Jiang et al., 2017). MSCs have been accepted to provide immunomodulatory effects in allogeneic, syngeneic, and even xenogeneic scenarios (Kao and Thomas, 2016; P De Miguel et al., 2012) as well as CSCs also have the ability to suppress T-cell-mediated tissue rejection which is aimed to be immune privilege (Du et al., 2009). Therefore, they become to prospect an effective therapeutic device and accomplished candidates in corneal bioengineering applications to generate normal transparent corneal stroma instead of pathogenic corneal lesion.

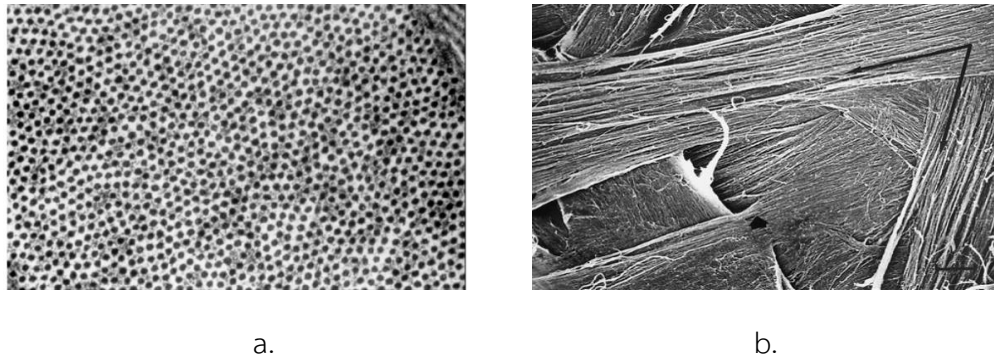


*Figure 2: Parallel orientation of collagen fibrils in lamella collagen stroma, transverse section (Robert et al., 2001) (a), and perpendicular alignment of each collagen lamellae (Meek and Fullwood, 2001) (b).*

## **Part 2 Tissue engineering**

### **2.1 Definition of Tissue Engineering**

Tissue engineering is arisen for recovery of the irreversible tissue damage which is the impact issues of human around the world. Its formal definition is “Tissue engineering is an interdisciplinary field that applies the principles of engineering and of life science towards the development of biological substitutes that restore, maintain, or improve tissue or organ function” (Langer R, 1993). The principle of tissue engineering is to evolve the manufactured tissue which has a capacity to transplant and consolidate in defected tissue through facilitate the normal tissue healing with absence of adverse effects. Tissue engineering composes of two main components, cells and carriers. Generally, firstly, the isolated cells are expanded and seeded in the manufactured scaffold or carrier before culturing in the static culture condition or dynamic bioreactor.

By way of corneal engineering, corneal substitution is developed, based on the fabrication of structural and functional requirements mimicking native cornea including transparency, biocompatibility, elasticity and tensile strength resemble to corneal, high optical transmittance, allowing the diffusion of nutrients, suitable mechanical toughness, appropriate biodegradability, less inflammatory response, clinical

compliance and providing for cell attachment, proliferation and differentiation (Carlsson et al., 2003).

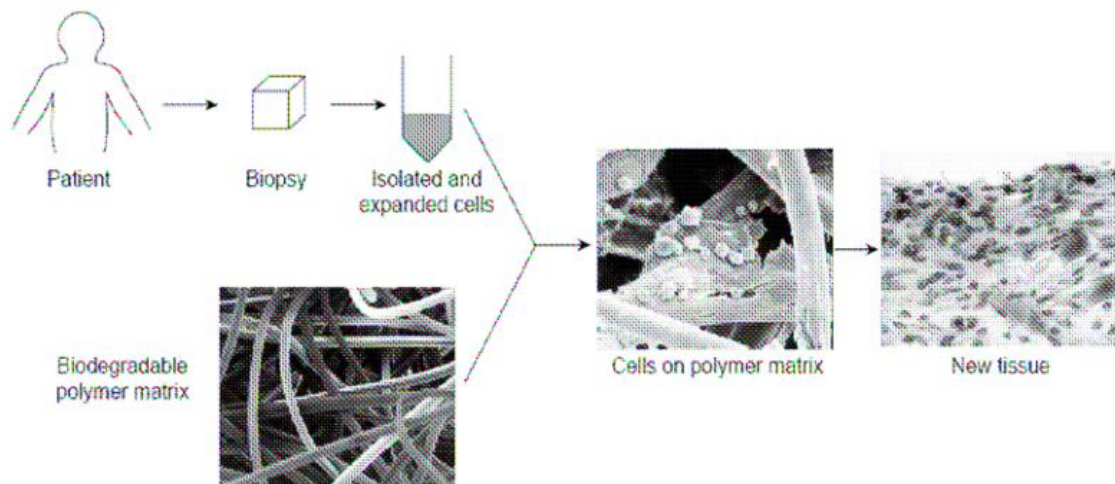


Figure 3: A common methodology of tissue engineering (Kim and Mooney, 1998)

## 2.2 Corneal cell Sources for Tissue Engineering

Cell sources can be divided into three types including autologous, allogenic and xenogenic. However, autologous cells are the most favored source due to their low risk of immune response. Nowadays, stem cells become to be used as a cell-based therapy together with suitable biomaterials because of their plasticity and self-renewal.

In corneal engineering, 3 cellular layers (epithelium, stroma and endothelium) comprised of 3 distinct cells (epithelial cell, keratocyte and endothelial cell respectively). Epithelial stem cells are located at corneoscleral limbus area, so called limbal epithelial stem cells (LESCs) that have a potential to generate corneal epithelial which are the terminal differentiated cells. LESCs have been used to treat limbal stem cells deficiency in humans by obtaining LESCs from unaffected fellow eyes (Keivyon and Tseng, 1989) as well as cadaveric donors eyes (de Araujo and Gomes, 2015; Tsai and Tseng, 1994). In last decade, keratocyte progenitor cells, corneal human stromal stem cells (hCSCs), have been discovered in corneoscleral rim with the properties of

stem cells including self-renewal, extended lifespan and ability to differentiate into specific cells, in particular keratocytes (Du et al., 2005). Especially, in floating pellets, hCSCs express corneal-like ECM with lamella collagen fibrils similar to corneal pattern and significantly improve more similarity of collagen alignment in nanofiber culture (Wu et al., 2012). Moreover, CSCs, *in vivo*, have been determined to subside the problems of corneal wound (Basu et al., 2014), corneal scarring (Hertsenberg et al., 2017) and stromal neovascularization and inflammation (Almaliotis et al., 2015). In other words, CSCs have superiority for being a cell source in stromal engineering. The last one is endothelial cells, unlike epithelium, endothelial cells are in non-proliferative stage with diminishing in cell number in time by age (Bourne et al., 1997; Joyce, 2005). However, there are some evidences of progenitor cells, but not stem cells, located in the area of posterior limbus, the transitional area between the periphery of the endothelium and Schwalbe's line to the anterior portion of the trabecular meshwork, thus these progenitor stem cells are able to generate both endothelial cells and trabecular cells (Yu et al., 2011).

### 2.3 Tissue Engineering Scaffolds

A tissue engineering scaffold can be categorized in structure as 2-D or 3-D and in material as synthetic or natural origin. Materials are usually used in polymer, generally, natural polymers are prominent in biocompatibility but synthetic polymers have more customization of the desired properties. Moreover, those of the materials can be modified to fulfill a preferable requirement such as controllable biodegradability, mechanical strength and high porosity for increasing cell migration and transferring nutrients and wastes. For a porous structure, there are mentioned the several ways to fabricate, basically, porogen-leaching, gas foaming, freeze-drying, fiber bonding, and phase separation (Ma, 2004). To increase cell attachment, proliferation and migration, modification of appropriate chemical (Ex. Arginine-glycine-aspartic acid (RGD), poly-L-lactic acid and peptide amphiphiles (PAs)) and generation of



topographical surface properties have been described (Karageorgiou and Kaplan, 2005; Leong et al., 2003).

In respect of corneal scaffold, natural scaffold for example collagen, silk, gelatin and chitosan and synthetic scaffold including poly (vinyl alcohol) (PVA), poly (2-hydroxyethyl methacrylate) (PHEMA), polyethylene (glycol) diacrylate (PEGDA), poly(lactic-co-glycolic acid) (PLGA) and poly(ethylene glycol)/poly(acrylic acid) and (PEG/PAA)-based hydrogels have been reported as the one or more layer of corneal scaffold. According to this experiment was addressed to fabricate in 2 layers of cornea, epithelium and stroma with silk and gelatin scaffold, the detail of silk and gelatin was mentioned.

### 2.3.1. Silk fibroin (SF)

Silk fibroin (SF) is a structural protein derived from the cocoon of the silkworm (*Bombyx mori*). Its advantage is biocompatibility, processability, non-immunogenic response, controllable degradation rates and mechanical properties, hence it has been used in tissue engineering and regenerative medicine. SF can be processed in many formed structures for example native fiber, electrospun fibers, films, sponge scaffold, hydrogels and microsphere by simple evaporation as well as electrospinning (Kundu, 2014). Commonly, to obtain SF solution, the precursor of the silk framework is mixed with lithium bromide solution before dialysis. The modulation of silk fibroin has been addressed to control material properties and adjust degradation rate which are the superior advantage than the other materials ex. collagen, chitosan and alginate. Secondary protein structure (alpha-helices and beta sheets) can be modulated through post-processing techniques including mechanical stress, heat, water and organic solvent (Agarwal et al., 1997; Gupta et al., 2007; Jin et al., 2005; Lu et al., 2010). Consequently, degradation rate, hydrophobicity/hydrophilicity, mechanical strength, transparency, porosity, oxygen permeability and thermal stability can be regulated (Horan et al., 2005; Jin et al., 2004; Motta et al., 2002). Water annealing, use of water vapor, is the most common use referred to control secondary protein structure with

up to 60% of beta sheet structure (Lawrence et al., 2008). Recently, a silk photocrosslinking method has been reported for changing silk physical property to be highly elastic and transparent hydrogel (Applegate et al., 2016; Ghezzi et al., 2015).

About corneal engineering, silk approaches the inherent optical clarity which has been used in human corneal limbal epithelial cells (HCLEs) similar to amniotic membrane (AM) which is a conventional substrate for corneal epithelium. However, lack of ECM in pure SF membrane, unlike AM, cell attachment property is subordinate (Bray et al., 2011). Remarkably, chemical modification by RGD sequence on the surface of silk membrane elevates the proliferation and attachment of HCLE cells, human keratocytes (Gil et al., 2010a; Lawrence et al., 2009) and human corneal endothelial cells (Madden et al., 2011). Moreover, this chemical modification also maintained its integrity and transparency for a half year with low immunogenic and low neovascular responses in rabbit stroma (Wang et al., 2015). For both corneal epithelial and stromal layers, porous silk film had an evidence to enhance the construction as well as synthesis corneal-like ECM by hCSCs (Bray et al., 2012; Gil et al., 2010b). The ability of permeability and biodegradability was presented in polyethylene glycol (PEG) inducing porous SF, but high porosity was investigated to be more vulnerable and faster degradation rate (Gil et al., 2010b; Higa et al., 2011; Suzuki et al., 2015). Furthermore, topographic modification, including the depth and width of grooves, stack patterned porous silk film or sponge, was effected on cell adherence, lamellae and the thickness of tissue (Ghezzi et al., 2015).

In this regard, silk fibroin can be considered as a preferable engineering material owing to the ability to modify in the large range of material processing windows and accessible methods for controlling the protein formation. Moreover, SF approaches the profound effects on the cell behavior, in particular, corneal cells.

### 2.3.2 Gelatin

Gelatin is a ubiquitous natural water-soluble protein derived from collagen hydrolysis. Comparing with collagen, gelatin has same amino acid sequence but contains less tertiary structure resulting in higher aqueous solubility (Pahuja et al., 2012). Gelatin as to tissue engineering generally implicates through crosslinking including chemical crosslinking such as glyceraldehyde (Sisson et al., 2009), glutaraldehyde (GA) (Talebian et al., 2007), polyepoxides (Nishi et al., 1995), natural products such as genipin (Bigi et al., 2002) and carbodiimide coupling (Kuijpers et al., 2000), enzymatic crosslinking such as microbial transglutaminase (mTG) (Yung et al., 2007), physical crosslinking such as plasma (Prasertsung et al., 2013), UV radiation (Bhat and Karim, 2009; Brinkman et al., 2003) and dehydrothermal treatment (DHT) (Ratanavaraporn et al., 2010; Watanabe et al., 2011). Physical crosslinking has a dominant advantage with non-chemical toxicity. Because of its lower immunogenicity, cost, aqueous solubility, containing with RGD sequence and ability to crosslink and process, gelatin becomes an excellent candidate for ocular tissue engineering (Katagiri et al., 2003; Prakashan, 2005).

In ocular tissue engineering, gelatin prepared by dehydrothermal was found the superiority in transparency, elastic modulus and albumin permeability. Seeding with primary human corneal endothelial cells on gelatin has been illustrated a continuous endothelial monolayer. (Watanabe et al., 2011). In chemical crosslinking, LESC, chitosan and gelatin crosslinking with glutaraldehyde were able to sustain more stem-like phenotype than tissue culture plate (Zhu et al., 2006). The incorporation with chondroitin sulfate (CS) has been exhibited primary rabbit corneal keratocytes (RCKs) cell growth, lower Young's modulus and resistance against protease digestion (Lai, 2013). Using of hyaluronic acid (HA) functionalized gelatin microspheres for 3-D culturing system with rabbit corneal keratocytes (RCKs) has been showed to maintain RCKs cell growth and tolerate in the anterior chamber of the rabbit eye (Lai and Ma, 2017). Glutaraldehyde crosslinked gelatin matrix together with stromal cells were

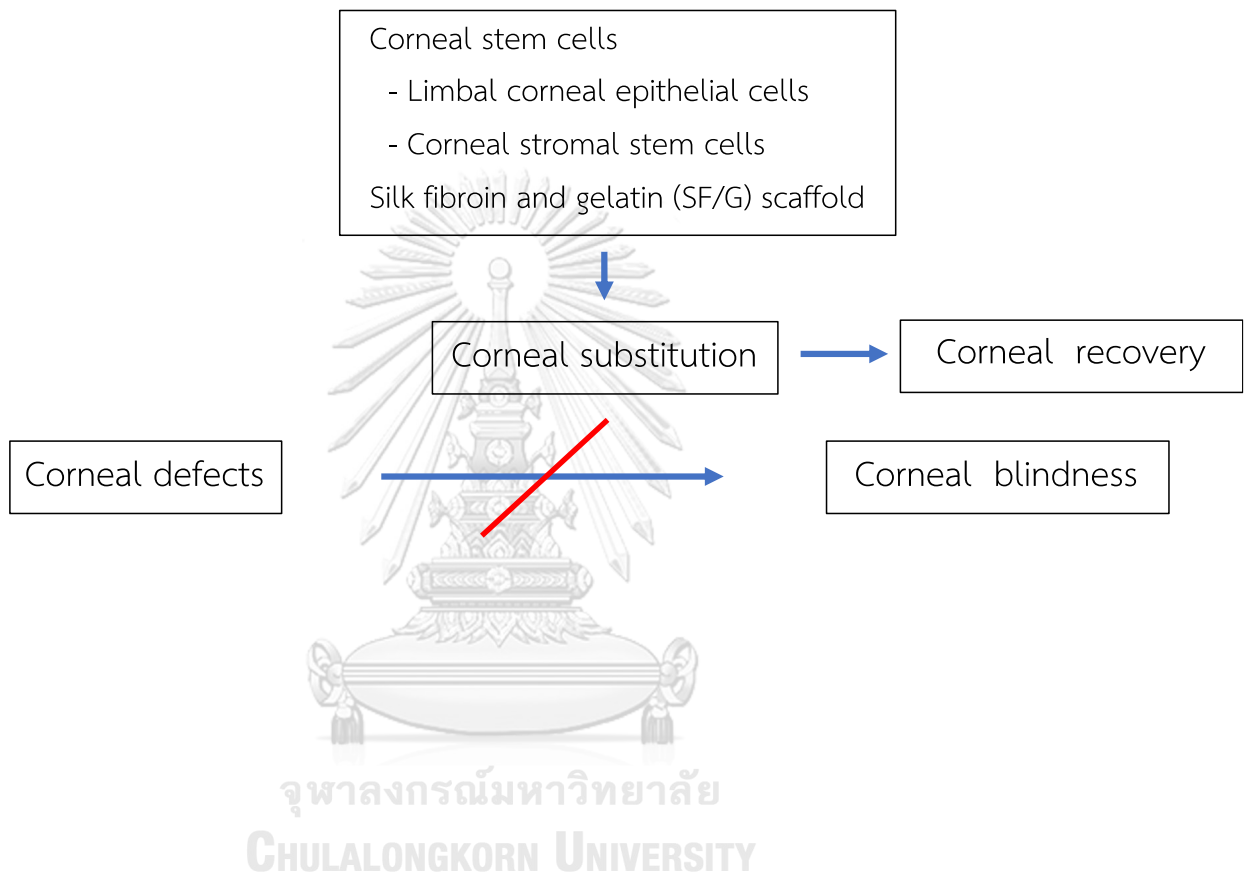
cultured as spheroids to reconstruct rabbit corneal stroma by implantation to corneal stromal pocket. After 4 weeks, keratocytes displayed desirable surface markers by histological immunostaining without evidence of immune cell infiltration (Mimura et al., 2011). Moreover, regarding to scaffolds with instructive topographies, in keratocyte and epithelial cells, gelatin based electrospun membrane with fiber alignment affected on better cell proliferation and biomarker presentation compared to random fiber orientations (Gao et al., 2012; Wilson et al., 2012; Yan et al., 2012).

### *2.2.3 Silk fibroin/gelatin (SF/G) blended scaffold*

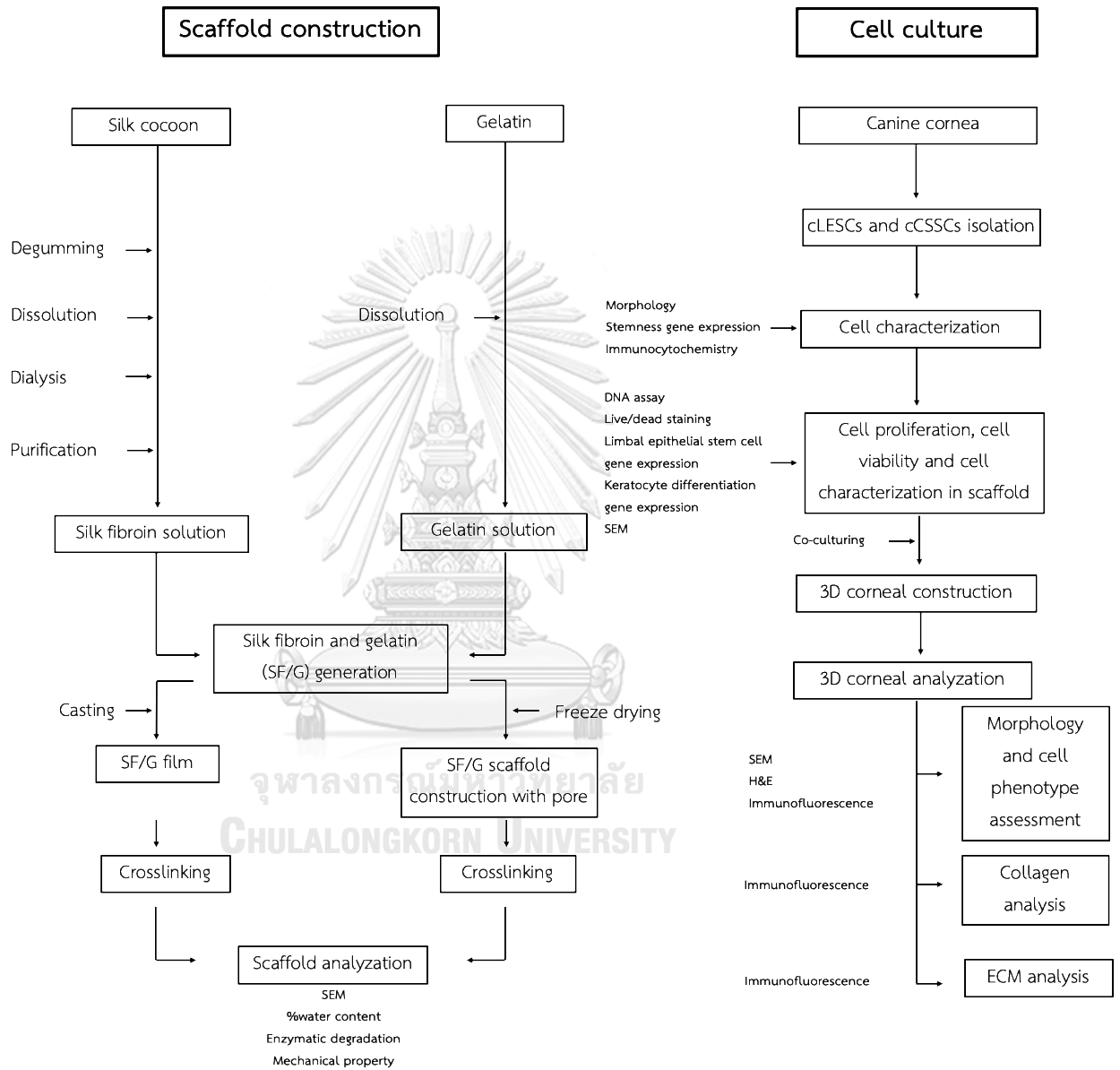
Silk fibroin has been performed as a scaffold with excellent mechanical property, biocompatibility but slow degradation rate and no RGD motif that is responsible for cell attachment. However, in the form of ocular surface bioengineering, scaffold is required no long-term degradation rate for avoiding ocular irritation. Incorporating with gelation, mixed of those components have been revealed to accelerate degradation rate, improve tensile strength, diminish inflammatory reactions and improve cell adhesion (Yang et al., 2012). It has been investigated to increase their properties of cell adhesion, proliferation and appropriate mechanical property by using mouse embryonic fibroblasts (MEF) and mesenchymal stem cell (Fan et al., 2008; Moisenovich et al., 2014). For crosslinking, likewise the other materials, silk fibroin with gelatin can be performed through chemical crosslink ex. EDC/NHS treatments and physical crosslink ex. dehydrothermal (Tungtasana et al., 2010), those procedures displayed suitable degradation time and less immune response *in vivo* (Tungtasana et al., 2010).

Therefore, this study was the first determination of bio-fabricated cornea based SF/G scaffold by the way of canine ocular tissue engineering and comprehend isolation and culture protocol for canine limbal epithelial stem cells (cLESCs) and canine stromal stem cells (cCSCs) to construct suitable canine corneal synthesis pointing to use as a promising corneal graft for transplantation.

## Conceptual framework



Experimental plan



## CHAPTER III

### Materials and methods

#### 1. Preparation of silk fibroin solution (SF)

*B. mori* Thai silkworm “hybrid silkworm (J108 X Nanglai strain)” cocoons were kindly received from the Queen Sirikit Sericulture Center, Sisaket province, Thailand. To prepare silk solution, silk cocoons were degummed by boiling for 30 min in 0.02 M of Na<sub>2</sub>CO<sub>3</sub> solution (Ajax Finechem, Australia). The silk fibers were then rinsed with 5 liters of deionized water for 4-5 times and dried overnight. After that, autoclaving procedure, at 121 °C for 20 min, was performed for sterilization. The silk fibers were dissolved in 9.3 M of LiBr solution (Sigma-Aldrich Corporation, USA) at 60 °C for 4 h and dialyzed through the dialysis bag (MWCO 12000-16000, Vikase Company Inc., Osaka, Japan) against distilled water (DI) for 3 days. After the conductivity of dialysate was similar to DI. Impurity was removed by centrifugation at 9,000 RPM (approximate 12,700 g) 4 °C for 20 min twice. The obtained SF solution was in a range of 6–7% w/w. (Chantong et al., 2019; Hu et al., 2011). Before using, SF solution was diluted with DI to 5% w/w.

#### 2. Preparation of gelatin (G)

The type A gelatin (Nitta Gelatin Co., Japan) (MW = 100,616) was kindly provided. 5% w/w of gelatin was prepared with 5g gelatin A and 100 g of DI. The solution was mixed by stirring in 40°C until homogeneous.

#### 3. Preparation of Silk fibroin/gelatin (SF/G) films

Silk fibroin/gelatin (SF/G) solution at a ratio of 30/70 and final solid concentration of 5% w/w was prepared by gently stirring for 10 min at room temperature (RT). Then, A 2 mL of mixed solution was cast in 5x5 cm of squamous polystyrene tray and dried in laminar hood overnight to obtain SF/G films. The SF/G

films were cut in circular shape with 1 cm diameter by sterile biopsy punch (Miltex, USA) and annealed in water filled desiccators under vacuum for 24 h for changing to insoluble form ( *$\beta$ -sheet structure*) of silk fibroin. The films were sterilized by gas plasma before use.

#### 4. Preparation of Silk fibroin/gelatin (SF/G) scaffolds

The SF/G solution at a ratio of 30/70 and final solid concentration of 5% w/w was prepared by gentle stirring for 10 min at RT. Then, the solution was cast on 5x5 cm of squamous polystyrene tray and created porous scaffolds by freezing at  $-80^{\circ}\text{C}$  overnight before lyophilization at  $-70^{\circ}\text{C}$  for 48 h. After that, SF/G scaffolds were crosslinked by dehydrothermal technique at  $140^{\circ}\text{C}$  for 72 h under vacuum in a vacuum oven. Air interphase area of scaffolds was removed prior to constructing in circular shape with 1 cm diameter by sterile biopsy punch (Miltex, USA) and slid in 1 mm thickness using microtome blade. The scaffolds were sterilized by gas plasma before use.

#### 5. Material morphological and structural characterization

To assess SF/G films, SF/G scaffolds, cLESCs seeded SF/G films, cSSCs seeded SF/G scaffolds and bio-fabricated cornea, scanning electron microscopy (SEM) was used to analyze the pore size pattern, surface, thickness, cell morphology, and overall structure. Dried samples (SF/G films, SF/G scaffolds) were sputtered by gold before SEM imaging. The thickness of materials and pore size were measured by ImageJ (US National Institute of Health, NIH). Whilst, wet samples (cLESCs seeded SF/G films, cSSCs seeded SF/G scaffolds and bio-fabricated cornea), before coating with gold, were fixed with 2.5% glutaraldehyde. For dehydration, ethanol series at  $4^{\circ}\text{C}$ . and critical point dry were processed to the last dehydration. SEM imaging analysis was performed by JEOL InTouchScope™ series SEMs, the JSM-IT500HR using 10 kV for all magnifications.



## 6. Swelling test

For water absorption capacities of SF/G films and SF/G scaffolds, swelling was processed. Dry form of SF/G films and SF/G scaffolds were weighted and immersed in DI water at specific time point. Before weighting, materials were blotted with paper to remove excessive water. The water content was then calculated by the following equation.

$$\text{Water absorption} = (M_t / M_0) / M_t \times 100\%$$

Where  $M_0$  is the initial weight of materials and  $M_t$  is weight of wet form at specific time point.

## 7. *In Vitro* enzymatic degradation



In vivo degradation tests were evaluated the degradation rate of SF/G films and SF/G scaffolds at specific time points. Briefly, SF/G films and SF/G scaffolds were incubated in 1U/ml of protease XIV solution (pH 7.4) (Sigma-Aldrich Corporation, USA) containing 0.01% w/v sodium azide (Loba Chemie PVT. LTD., India) for antimicrobials at 37°C and replaced every two days. Hereafter, the remained materials were washed with DI and centrifuged at 10000 RPM for 5 min to remove non-material solution for 3 times. Materials were dried at 60 °C in heating block overnight. Then, the dried form of materials was weighted and normalized according to following equation.

$$\text{Residual mass (\%)} = W_t / W_0 \times 100\%$$

Where  $W_0$  is the initial weight of materials and  $W_t$  is the weight of materials at specific time point.

## 8. Uniaxial tensile test

Shimadzu universal testing machine was performed to determine tensile strength conforming under a crosshead speed of 5 mm/min until ultimate failure. 40  $\mu\text{m}$  thickness of SF/G films and 1 mm thickness of SF/G scaffold were cut into dumbbell shape with 2 cm of gag length and 1-cm width and immersed in PBS until equilibrium. 4 identical samples of each material were analyzed. The ultimate tensile

strength (UTS), elastic modulus (Mpa) and elongation values at break were automatically calculated.

## 9. Canine limbal corneal epithelial cell (cLECs) isolation and culture

This project underwent canine cadaveric cornea, so it was not applicable for IACUC approval. Unilateral/Bilateral corneas were obtained from fifteen cadaveric healthy dog eyes (age between 1 to 7 years old) without pathological lesion of the eyes and less than 4 h of preservation. Collected corneas were transported in transport media including Dulbecco's modified Eagle's medium (DMEM; Thermo Fisher Scientific Corporation) with 10% Fetal bovine serum (FBS; Thermo Fisher Scientific Corporation) at 4 °c. For preparation, corneas were rinsed with Hank's Balanced Salt solution (HBSS) (Thermo Fisher Scientific Corporation) containing with 100 unit/mL penicillin (Thermo Fisher Scientific Corporation), 100 µg/mL streptomycin (Thermo Fisher Scientific Corporation), 5 µg/mL amphotericin B (Thermo Fisher Scientific Corporation) and gentamycin 50 µg /mL (Thermo Fisher Scientific Corporation) for six times. After removing the excessive tissue, corneas were dissected at the superficial limbal area into 8 pieces equally by crescent knife (Alcon, USA) and corneal scissors and incubated in collagenase I (Sigma-Aldrich Corporation, USA) 0.5 mg/mL for 16h 37°C. After that, epithelial cells were dissociated by cell scraper at the epithelial side and pipetting to create single cell suspension. Cell suspension was then added to 4 times volume of Dulbecco's modified Eagle's medium (DMEM; Thermo Fisher Scientific Corporation) with 10% Fetal bovine serum (FBS; Thermo Fisher Scientific Corporation) and collected by centrifugation. The isolated cells were seeded on the prepared plate with mitotically inactive 3T3 J2 fibroblast. Limbal epithelial stem cell media containing with high glucose Dulbecco's Modified Eagle Media: Nutrient Mixture F-12 (DMEM /F-12; Thermo Fisher Scientific Corporation) supplemented with 10% fetal bovine serum (FBS; Thermo Fisher Scientific Corporation), 2 mM L-glutamine (100x GlutaMAX™; Thermo Fisher Scientific Corporation), 100 unit/mL penicillin (Thermo Fisher Scientific Corporation), 100 µg/mL streptomycin (Thermo Fisher Scientific Corporation), and 5 µg/mL amphotericin B (Thermo Fisher Scientific Corporation), 20 ng/mL human

recombinant epidermal growth factor (EGF; Milipore Corporation), 1x insulin-transferrin-selenium (ITS; Invitrogen) and 0.5 µg/mL hydrocortisone (Sigma-Aldrich Corporation, USA) was used for culture at 37 °C under 95% humidity and 5% CO<sub>2</sub>. Media were substituted every 2 days. Cells in the passage 3 were accessed to further experiments. For cLESCs expanding, mitotically inactive 3T3 J2 fibroblasts were used as a feeder cell. Before subculture, 3T3 J2 fibroblasts were removed by 1 min trypsin incubation whereas cLESCs were used more than 5 min trypsin incubation.

#### 10. Preparation of 3T3 feeder cells

3T3 J2 fibroblast cells were kindly given from *Stem Cell and Cell Therapy Research Unit, King Chulalongkorn Memorial Hospital*. *As feeder cells, 3T3 J2 fibroblast cells have an ability to improve cell proliferation and sustain stem/progenitor cells in corneal epithelial cells (Nam et al., 2015)*. After confluence, 3T3 was inhibited the proliferation by 10 µg/mL of mitomycin C (Sigma-Aldrich corporation, USA) for 2h at 37 °C under 5% CO<sub>2</sub> and washed with PBS 2 times before seeding cLESCs.

#### 11. Canine corneal stromal stem cells (cSSCs) isolation and culture

Canine corneal stromal stem cells (CSSCs) were isolated after removing limbal epithelial stem cells. The remaining limbal tissues were cut into smaller pieces and scrapped with a cell scrapper (SPL Lift Sciences, Korea). Then, the tissues and cell suspension were filtered through 70 µm cell strainer (SPL Lift Sciences) and centrifuged to obtain cell pellet. The pellet was resuspended and seeded in 60 mm culture plate. Corneal stromal stem cell proliferation media contained with DMEM/MCDB-201 (Sigma-Aldrich corporation, USA) in the ratio of 1:1 (v/v), 2% fetal bovine serum, 10 ng/mL platelet-derived growth factor (PDGF-BB; Millipore corporation), 10 ng/mL epithelial growth factor (EGF; Millipore corporation), 0.1 mM ascorbic acid, 10<sup>-8</sup> M dexamethasone, 1x insulin-transferrin-selenium (ITS; Invitrogen) was used to culture at 37 °C under 5% CO<sub>2</sub>. Cells were then subcultured when they reach the confluence. The third passage was used in further experiment.

## 12. Keratocyte differentiation

cSSCs at the third passaged were seeded into SF/G scaffold at the concentration of  $6 \times 10^6$  cells/mL; 80  $\mu$ l. After 3 days, the media were changed from corneal stromal stem cell proliferation media to keratocyte differentiation media (KDM) consisted of DMEM (Thermo Fisher Scientific Corporation) supplemented 1.0 mM L ascorbic acid-2-phosphate (Sigma-Aldrich Corporation, St Louis, USA), 2 mM L-glutamine (100x GlutaMAX™; Thermo Fisher Scientific Corporation), 100 unit/mL penicillin (Thermo Fisher Scientific Corporation), 100  $\mu$ g/mL streptomycin (Thermo Fisher Scientific Corporation), and 5  $\mu$ g/mL amphotericin B (Thermo Fisher Scientific Corporation), 10 ng/mL basic fibroblast growth factor (FGF-2, Millipore corporation) and 0.1 ng/mL transforming growth factor-beta3 (TGF- $\beta$ 3, Sigma-Aldrich Corporation, USA) and continuously cultured.

## 13. Quantitative reverse transcription PCR (RT-qPCR)

RT-qPCR was performed to characterize both cLESCs and cSSCs at passage 3, 14 days after culturing in tissue culture plates (TCP). cLESCs seeded on SF/G film and cSSCs seeded into SF/G scaffold were executed at day 14 and day 28. Briefly, RNA was collected by using TRIzol-RNA isolation reagent (Thermo Fisher Scientific Corporation, USA) following by extracting with DirectZol-RNA isolation kit (ZymoResearch, USA) according to the manufacture's protocol. ImProm-™ Reverse Transcription System (Promega, USA) was used for converting total RNA to cDNA. The targeted genes were amplified by FastStart Essential DNA Green Master (Roche Diagnostics) using CFX96™ real-time PCR detection system (Bio-Rad). The groups of primers are presented in table 1.

In this experiment, glyceraldehyde 3-phosphate dehydrogenase (*Gapdh*) was appointed to be a reference gene. The gene expression levels were normalized by *Gapdh* and calculated from this formula:  $2^{-\Delta\Delta CT}$ , where  $\Delta\Delta CT = [C_t^{\text{target gene}} - C_t^{\text{GAPDH}}]$

treated -  $[Ct^{\text{target gene}} - Ct^{\text{GAPDH}}]_{\text{control}}$  (Ct referred to cycle threshold). In each experiment, gene expression was analyzed from 4 subjects.

**Table 1: Primer sequences**

Gene	Accession number	Sequences	5' 3'	Length (bp)	Tm (°C)
<b>Stemness genes</b>					
<i>Rex1</i>	XM_0036395	Forward	AGGTTCTCACAGCAAGCTCA	199	59.24
	67.1	Reverse	CCAGCAAATTCTGCGCACTG		60.73
<i>Oct4</i>	XM_538830.1	Forward	AGGAGAAGCTGGAGCAAAC	100	60.55
		Reverse	GTGATCCTCTTCTGCTTCAGG		59.50
<b>Mesenchymal stemness marker</b>					
<i>CD90</i>	NM_0012871	Forward	AGGACGAGGGGACATACACA	109	59.69
	29.1	Reverse	ATGCCCTCACACTTGACCAG		59.69
<b>Proliferation marker</b>					
<i>Ki67</i>	XM_0141087	Forward	GTGCAACTAAAGCACGGAGA	124	58.49
	88.1	Reverse	GAGATTCCTGTTTGCGTTTTTC		59.49
<b>Limbal stem cell marker</b>					
<i>P63</i>	XM_856275.3	Forward	CTGGAGCCAGAAGAGAGGAC	102	60.89

		Reverse	CGTGACTGTGGCTCACTAAA	60.14
<i>Abcg2</i>	NM_0010480	Forward	CAGGGCTGTTGGTAAATCTCA	54.8
	21	Reverse	TACTGCAAAGCCGCATAACC	56.0

---

**Corneal epithelial  
cell marker**

---

<i>Krt3</i>	NM_0013460	Forward	GTCAGCATCTCCGTGCTCAG	188	60.04
	12.1	Reverse	GCTGAAGCCTCCACCACTG		60.04
<i>Krt12</i>	NM_0010824	Forward	ATTGCCGAGCAGAACCGTAA	188	60.04
	21.1	Reverse	TCCAGGGATTTCTTCGTGGC		60.04

---

**Corneal stromal  
stem cell marker**

---

<i>Nes</i>	XM_014115	Forward	CAGCAGCTAGCACACCTCAA	141	60.32
	306.2	Reverse	CTCCAGTTTAGGGTCCTGGAA		58.73
<i>Pax6</i>	NM_0010975	Forward	CCCAGTATAAGCGGGAGTGC	144	60.25
	44.1	Reverse	GTTGCTTTTCGCTAGCCAGG		59.83
<i>Ngfr</i>	XM_022423	Forward	CAGCAGCTAGCACACCTCAA	141	60.32
	913	Reverse	CTCCAGTTTAGGGTCCTGGAA		58.73

---

**Keratocyte marker**

---

<i>Kera</i>	XM_847392	Forward	GTGAGGTGCTGTCGTTGTTG	172	59.70
	.4	Reverse	TGCCATGATAGTACCTCAGCC		59.31

<i>Aqp1</i>	NM_001003	Forward	GCATCGAGATCATTGGCACC	144	59.41
	130.1	Reverse	CTGTGTAGTCGATCGCCAG		57.76
<i>Aldh3a1</i>	NM_001082	Forward	TTCAACTCGGGCAAGACTCG	134	60.32
	420.1	Reverse	GCGTTCCACTCATTCTTGTGC		60.40
<i>Lum</i>	XM_539716.	Forward	TCCGTCCTGACAGAGTTCAC	111.	59.04
	6	Reverse	TGGCAAATGCTTTGAATCCTTC		58.07
<b>Myofibroblast marker</b>					
<i>Acta2</i>	XM_534781	Forward	CCATGAAGATCAAGATCATTGC	176	57.88
	.6	Reverse	ACAGAGCAAGGAAGCGTCT		58.95
<b>Reference gene</b>					
<i>Gapdh</i>	NM_001003	Forward	CCAACTGCTTGGCTCCTCTA	100	59.38
	142.1	Reverse	GTCTTCTGGGTGGCAGTGAT		59.67

#### 14. Cell proliferation assay

For cell proliferation, DNA of cLESCs seeded SF/G film (100,000 cell/cm<sup>2</sup>) and cSSCs seeded SF/G scaffold (cell concentration 6x10<sup>6</sup> cells/mL; 80  $\mu$ l/scaffold) were quantified at day 1, 3, 5, 7, 14 and 28. 4 replications of each time point were digested with 1.0 mg/ml proteinase K (Worthington Biochemical, USA) in proteinase K buffer (150 mM Tris HCl and 1 mM EDTA pH 8.0) and 20  $\mu$ l/sample of papain suspension

(Worthington Biochemical, USA). After that, all samples were incubated at 60 °C 16h in heating block. The centrifugation was performed with 8000 rpm for 10 min at 4°C. The supernatant was then transferred to the new tube. DNA level was measured by Qubit Fluorometric Quantification with dsDNA BR assay. For each sample, 1- $\mu\text{l}$  supernatant was combined with 199- $\mu\text{l}$  Qubit buffer and vortexed for homogeneity. Then, combined solutions were incubated for 2 min at RT. The Qubit Flex Fluorometer was used to quantify DNA level. Quantitative data was normalized with plain film and scaffold. Absorbance data were carried to present.

### **15. Cell viability assay and distribution**

Parallel to the time point of the cell proliferation assay, LIVE/DEAD cell double staining was illustrated by cLESCs seeded SF/G films and cCSCs seeded SF/G scaffolds. In brief, as the same cell concentration in proliferation assay, in 24 well plate, the samples were washed with HBSS (Thermo Fisher Scientific Corporation, USA) to remove nonspecific background. Before incubation with cell staining, calcein AM solution (Thermo Fisher Scientific Corporation, USA) and propidium iodide solution (Sigma-Aldrich Corporation, USA) were prepared by diluting with HBSS (1:1000 in HBSS; Thermo Fisher Scientific Corporation, USA) simultaneously. The staining solution was then added to well plates and incubated for 30 min at 37°C. After that, the solution was washed with HBSS (Thermo Fisher Scientific Corporation, USA) and observed under a fluorescent microscope incorporated with Carl Zeiss™ Apotome.2 apparatus (Carl Zeiss, Germany).

### **16. Bio-fabricated cornea formation**

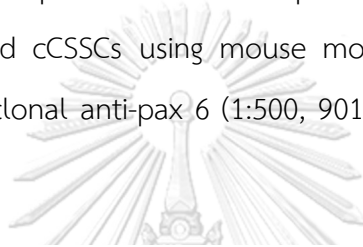
To mimic 3-D corneal structure, both materials were placed on a 12-well cell insert (translucent PET high pore density (HD); Falcon Corporation) separately. cLESCs were seeded at the density of 100,000 cell/cm<sup>2</sup> on the prepared SF/G films while cCSCs were seeded into SF/G scaffolds at the concentration of 6x10<sup>6</sup> cells/mL; 80



$\mu$ l. cLESCs were further cultured with limbal epithelial stem cell media containing with high glucose Dulbecco's Modified Eagle Media: Nutrient Mixture F-12 (DMEM /F-12; Thermo Fisher Scientific Corporation) supplemented with 10% fetal bovine serum (FBS; Thermo Fisher Scientific Corporation), 2 mM L-glutamine (100x GlutaMAX™; Thermo Fisher Scientific Corporation), 100 unit/mL penicillin (Thermo Fisher Scientific Corporation), 100  $\mu$ g/mL streptomycin (Thermo Fisher Scientific Corporation), and 5  $\mu$ g/mL amphotericin B (Thermo Fisher Scientific Corporation), 20 ng/mL human recombinant epidermal growth factor (EGF; Milipore Corporation), 1x insulin-transferrin-selenium (ITS; Invitrogen) and 0.5  $\mu$ g/mL hydrocortisone (Sigma-Aldrich Corporation, USA). Whereas cSSCs into SF/G scaffolds were cultured with corneal stromal stem cell proliferation media containing with DMDM/MCDB-201 (1:1 ratio; Sigma- Aldrich corporation, USA), 2% fetal bovine serum, 10 ng/mL platelet- derived growth factor (PDGF-BB; Millipore corporation), 10 ng/mL epithelial growth factor (EGF; Millipore corporation), 0.1 mM ascorbic acid,  $10^8$  M dexamethasone, 1x insulin-transferrin-selenium (ITS; Invitrogen) for 3 day for cell adhesion and proliferation. For attachment, tissue glue (Tisseel®; Baxter Corporation, USA) was applied on cSSCs seeded SF/G scaffolds. cLESCs seeded SF/G films were then gently transferred on the top and left in RT for 5 min to complete polymerization. Then, media were then added with keratocyte differentiation media consisted of DMEM (Thermo Fisher Scientific Corporation) supplemented 1.0 mM L ascorbic acid-2-phosphate (Sigma-Aldrich Corporation, St Louis, USA), 2 mM L-glutamine (100x GlutaMAX™; Thermo Fisher Scientific Corporation), 100 unit/mL penicillin (Thermo Fisher Scientific Corporation), 100  $\mu$ g/mL streptomycin (Thermo Fisher Scientific Corporation), and 5  $\mu$ g/mL amphotericin B (Thermo Fisher Scientific Corporation), 10 ng/mL basic fibroblast growth factor (FGF-2, Millipore corporation) and 0.1 ng/mL transforming growth factor-beta3 (TGF- $\beta$ 3, Sigma-Aldrich Corporation, USA) fully covered the whole scaffolds and further cultivated for 7 days. Hereafter, air lifting interface was generated to induce epithelial cell stratification. Media were resubstituted every 2 days until 4 weeks.

## 17. Histology, immunocytochemistry and immunohistochemistry

Routine H&E staining was manipulated to evaluate cell distribution with scaffolds. For immunocytochemistry preparation, P3 of cLESCs and cSSCs were seeded into chamber slide (SPL Life Sciences, Korea) with 5,000 cells/chamber and incubated at 37 °C under 95% humidity and 5% CO<sub>2</sub> for 24 h. Hereafter, the slides were fixed with 100% cold methanol for 15 min and permeabilized with 0.1% Triton X-100 (Sigma-Aldrich, Missouri, USA) for 10 min. To reduce non-specific background, 10% donkey serum in PBS was exploited for 1 h. The primary antibodies were incubated for characterized cLESCs and cSSCs using mouse monoclonal anti-p63 (1:50; ab735, Abcam) and rabbit polyclonal anti-pax 6 (1:500, 901301, BioLegend) respectively for overnight at 4 °C.



In term of immunofluorescence, cLESCs seeded SF/G films at day 14 and 28 were transferred to the chamber slide (SPL Life Sciences) and prepared for the procedure as above before incubated with primary antibodies. cSSCs seeded SF/G scaffold and bio-fabricated cornea at day 14 and 28 were washed with PBS and fixed in 4% paraformaldehyde. After dehydration with *alcohol*, samples were embedded in paraffin blocks and cut into 3- $\mu$ m-thick section by using a microtome and transferred to slides. After that, the sections were rehydrated in xylene and through descending graded series of alcohol. Twice of 5 min microwave heating (600 w) were performed in citric acid buffer (pH 6) for antigen retrieval. Hereafter, the sections were wash with PBS and blocked in 10% donkey serum in PBS for 1 h. Then, the sections were incubated with primary antibodies diluted with PBS and 1% bovine serum albumin (BSA; Sigma-Aldrich Corporation, USA) overnight at 4 °C. For primary antibody, to characterized and localized of cLESCs and differentiated keratocyte, mouse monoclonal anti-p63 (1:50; ab735, Abcam) and rabbit polyclonal anti-Aldh3a1 (1:200; ab129815, Abcam) were applied respectively. Extracellular matrix investigation, rabbit monoclonal anti-lumican (1:200; ab168348, Abcam) and rabbit polyclonal anti-collagen I (1:400; ab254113, Abcam) were used to determine lumican and collagen pattern and alignment. All the antibodies were incubated separated in adjacent sections.

For secondary antibodies, FITC-conjugated goat anti-mouse IgG H&L (1:1,000; ab6785, Abcam), Cy3-conjugated goat anti-rabbit (1: 500; minimal x-reactivity, BioLegend) were followed at RT in the dark room for 1h. DAPI was exploited to nuclear counterstain for investigating cell location and distribution. The sections were then mounted with Vecta Shied (Vector Laboratories Inc., Burlingame, CA). Isotype controls were served as negative control. For visualization, a fluorescent microscope incorporated with Carl Zeiss™ Apotome 2 apparatus (Carl Zeiss, Germany) was used.

### 18. Statistical analysis

Data analysis was represented as dot plot (N=4) using GraphPad Prism 9.0 (GraphPad Software, San Diego, CA) and statistical analysis was determined using SPSS statistics 22 software (IBM Corporation, USA). For comparison between 2 groups and more than 2 groups of continuous parameters, nonparametric tests were used with Mann-Whitney test and Kruskal-Wallis test respectively. The significance level was considered when  $p < 0.05$ . All experiments were run in at least quadruplicate for independent experiments.

## CHAPTER III

### RESULTS and DISCUSSION

#### Results

##### cLESCs and cCSCs isolation and characterization

cLESCs and cCSCs were successfully isolated from the canine cadaveric cornea with collagenase I. cLESCs were adhered and formed holoclones within 3 days after isolation. Cobble stone-like cell sheets surrounded with the area of interface and 3T3 inactive 3T3 J2 fibroblast were presented (Figure 1A). cLESCs exhibited stemness-related markers (*Rex 1* and *Oct4*) (Figure 1C), proliferation marker (*Ki67*) (Figure 1D), the limbal stem cell markers (*Abcg2* and *P63*) (Figure 1E) and corneal epithelial markers (*Krt3* and *Krt12*) (Figure 1F). cCSCs were also adhered to culture plate 2 h after seeding and reached 60-70% confluence within 7 days. The morphology was turned from oval shape to fibroblast-like appearance by culture time (Figure 1B). Gene expression of cCSCs indicated both adult and pluripotent stemness-related markers (*Rex 1*, *Oct4*, *Pax6*, *Ngfr*, *Nes* and *CD90*) (Figure 1G, J), proliferation marker (*Ki67*) (Figure 1H), genes associated with keratocyte (*Aldh3a1*, *Aqp1*, *Kera*, and *Lum*) (Figure 1K) and myofibroblast marker (*ACTA2*) (Figure 1I). Moreover, tumor protein P63 and the nuclear paired box protein Pax6 (oculorhombin) which are the marker of cLESCs and cCSCs respectively were presented by immunocytochemistry (Figure 1L, M) (Kafarnik et al., 2020; Nam et al., 2015). To summarize, the isolation of cLESCs and cCSCs was completed explained by genotypic and phenotypic characterization.

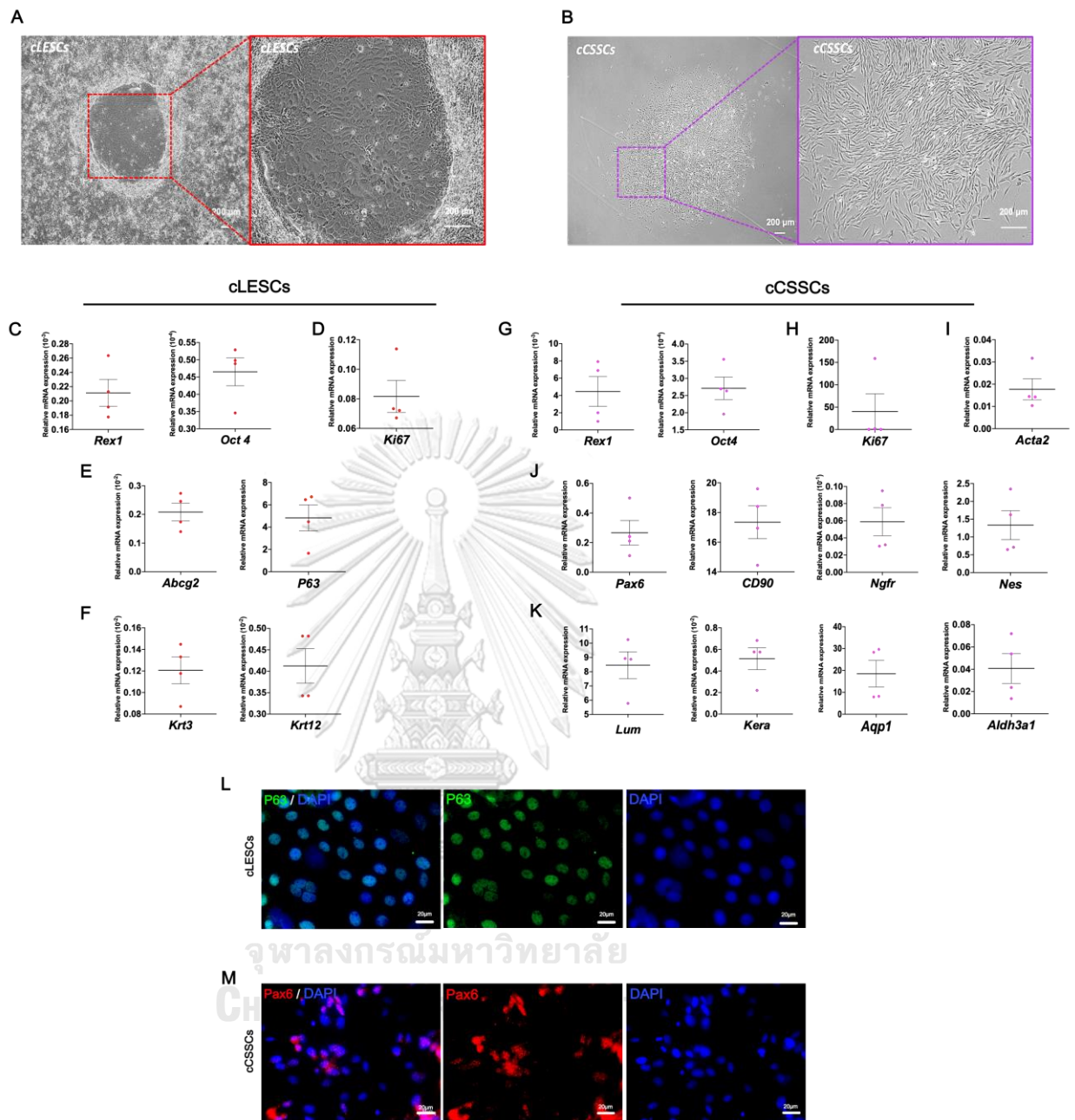


**Figure 4: cLESCs and cSSCs characterization.**

Morphological appearance of cLESCs (A) and cSSCs (B) are illustrated under a phase contrast microscope with 40x and 100x magnification. cLESCs and cSSCs mRNA expression are quantified by RT-qPCR and normalized by *Gapdh*. Pluripotent stemness-related markers (C, G), adult stemness-related markers (E, J), proliferation marker (D, H), epithelial cell markers (F), keratocyte marker (K) are characterized (n=4).

Immunocytochemistry of cLESCs and cSSCs expresses P63 and Pax6 respectively (L, M) with 400x magnification.

#### SF/G film and scaffold fabrication and characterization

In the matter of SF/G film, the substrate of cLESCs, was constructed by casting from 2- mL SF/G solution resulting in average 40  $\mu\text{m}$  thickness. The transparency of dry form and wet form were exhibited by weave texture pattern and color of the paper behind (Figure 2A, B). In comparison, wet form provided superior clarity due to water absorption (Figure 2B). From SEM evaluation, the surface of SF/G film was absolutely smooth and non-porous (Figure 2C). As regards the SF/G scaffold, the appearance showed white opaque coin-like shape (Figure 2D). However, after water equilibrium, transfiguration to white faded color was observed (Figure 2E). The proceeding of freeze drying achieved small pore production generalized of the material. The surface and cross sections were illustrated multiple pores and irregular surface topography. The pores were sharp edged with approximate  $130.71 \pm 37.12 \mu\text{m}$  diameter (Figure 2F). These results showed that SF/G was successfully fabricated to smooth surface films and porous sponge-like scaffolds.

**Table 2: Elastic Modulus, UTS, and % elongation at break**

Materials	Elastic modulus (Mpa)	UTS (Mpa)	Elongation (%)
SF/G film	$1.77 \pm 0.40$	$0.56 \pm 0.18$	$68.4 \pm 2.98$
SF/G scaffold	$1.25 \pm 0.91$	$0.18 \pm 0.09$	$2.63 \pm 0.58$

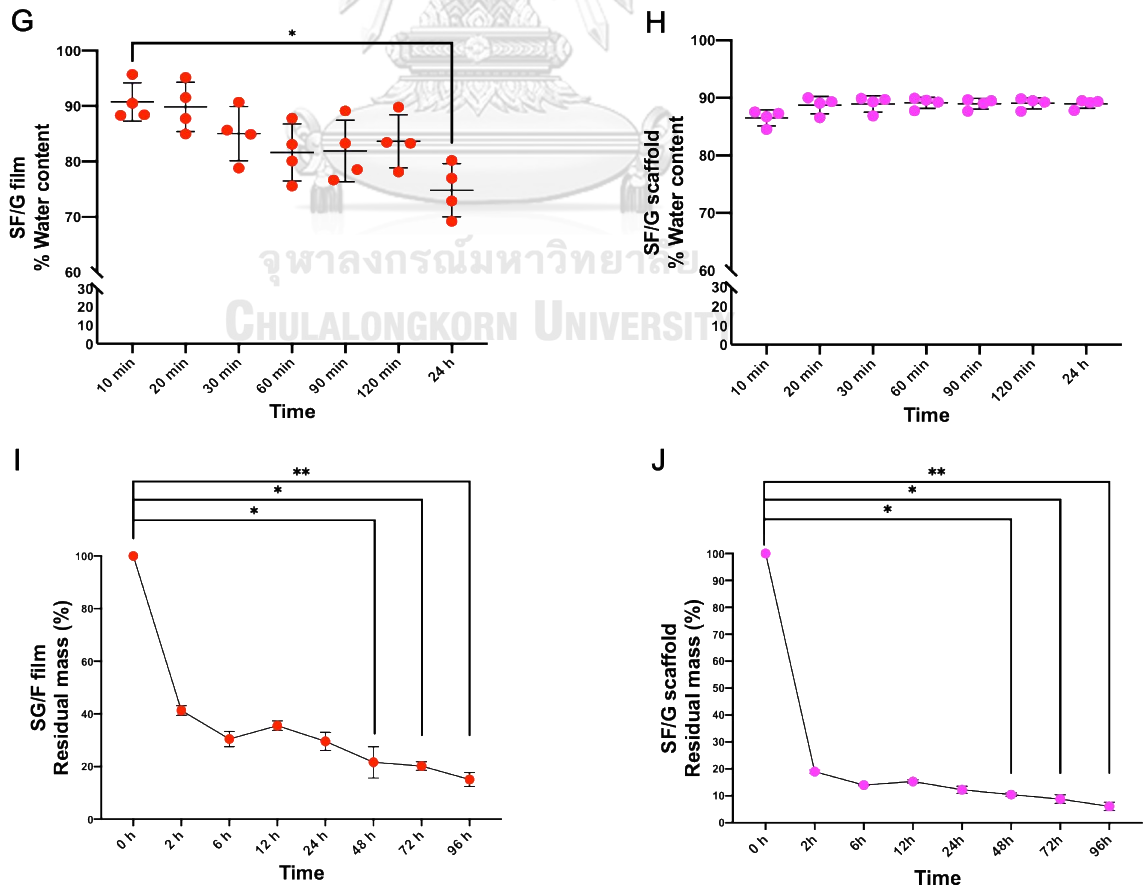
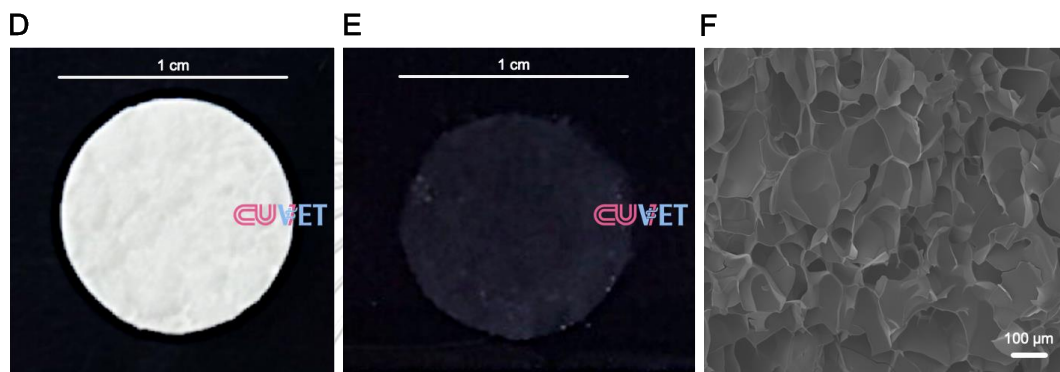
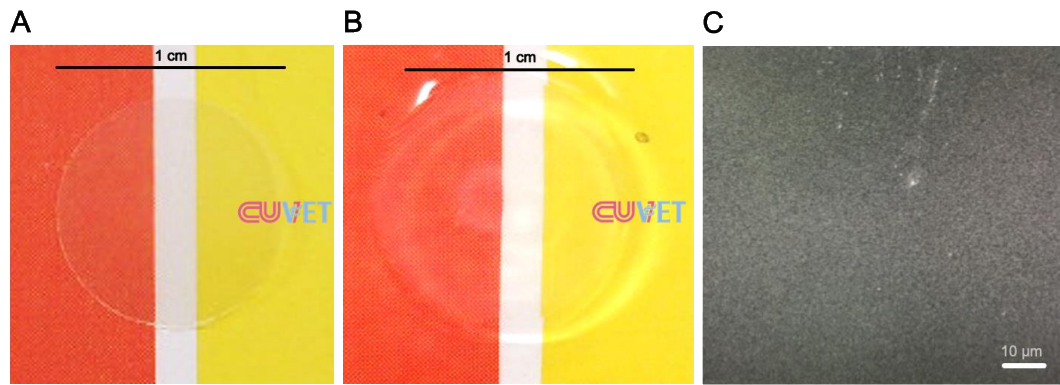


**Figure 5: SF/G film and scaffold characterization.**

External appearance of SF/G film in dry form (A) and wet form (B) as well as SF/G scaffold in dry form (D) and wet form (E) are illustrated. For ultrastructure features, scanning electron microscope shows smooth surface of SF/G film (1000x) (C). A 100x view of SF/G scaffold shows porous surface (F). Equilibrium of water content related to swelling capacity of SF/G film (G) and SF/G scaffold (H). Enzymatic *in vitro* degradation rate of SF/G film (I) and SF/G scaffold (J) using protease XIV solution. Data from four independent experiments ( $n = 4$ )  $\pm$  standard deviation (\* $p < 0.05$ , \*\* $p < 0.01$ ).

Physical properties of SF/G film and Scaffold

The imperative factors for corneal tissue materials have been included swelling property, transparency, degradation rate and suitable mechanical strength. The swelling tests of SF/G films were exhibited beyond 90% of water content and gradually decreased at any time points until significant difference at 24 h ( $p < 0.05$ ) (Figure 2G). Whilst SF/G scaffold had a capacity to sustain %water content further than 85% and no significant difference at all time points (Figure 2H). *In Vitro* enzymatic degradation manifested less than 50% of residual mass in both materials within 2h. For SF/G film, % residual mass was between 20-40% during 6h to 72h and less than 20% at 96h (Figure 2I). Besides, SF/G scaffold, % residual mass remained 10-20% after 2h up to 48 h after that almost entirely degraded, less the 10% (Figure 2J). The significant differences were showed between initiated time point and 48 h ( $p < 0.05$ ), 72h ( $p < 0.05$ ) and 96h ( $p < 0.01$ ) in both materials (Figure 2I, J). Mechanical testing determined tensile characteristics of both materials, the result revealed remarkable differences described by elastic modulus, ultimate tensile strength value (UTS) and % elongation at break. The elastic modulus of SF/G scaffolds, UTS and % elongation at break showed lower than the other. However, the significant differences were not noticed (Table 2).



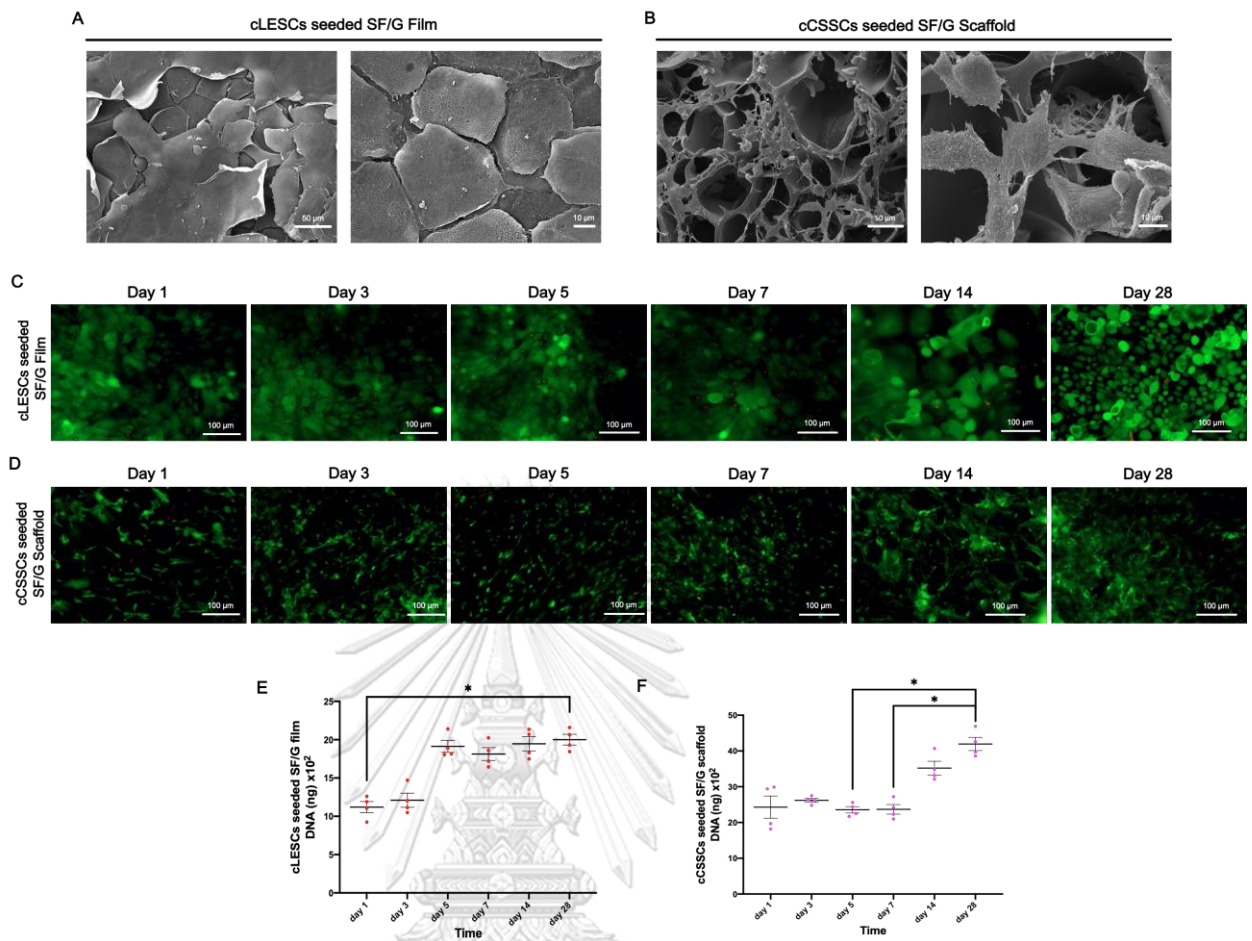
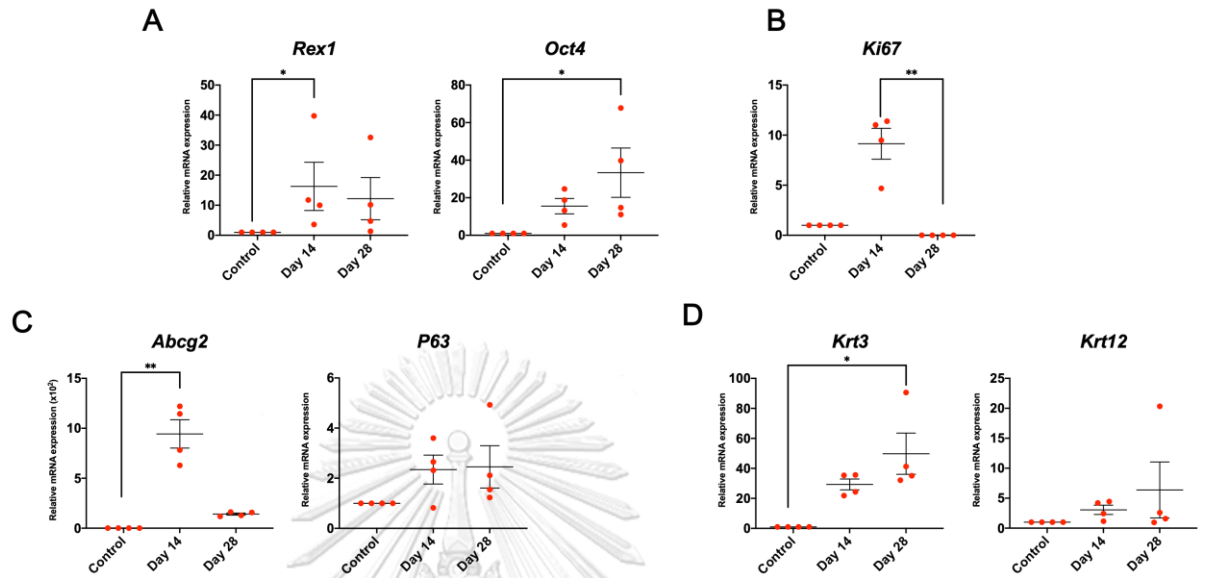


**Figure 6: cLESCs seeded SF/G film and cCSCCs seeded scaffold.**

Scanning electron microscope (SEM) images of cLESCs seeded SF/G film (350x and 1000x) (A) and cCSCCs seeded SF/G scaffold (350x and 1500x) (B) after 14 days of culturing. Fluorescent images of live/dead staining of cLESCs seeded SF/G film (C) and cCSCCs seeded SF/G scaffold (D) at day 1, 3, 5, 7, 14 and 28. Cell proliferation assay shows the proliferation pattern of cLESCs seeded SF/G film (E) and cCSCCs seeded SF/G scaffold (F) at day 1, 3, 5, 7, 14 and 28 (100x magnification). All the data are expressed as means  $\pm$  standard error of mean (SEM) (n=4) (\* $p < 0.05$ ).

## cLESCs seeded SF/G film



## cSSCs seeded SF/G scaffold

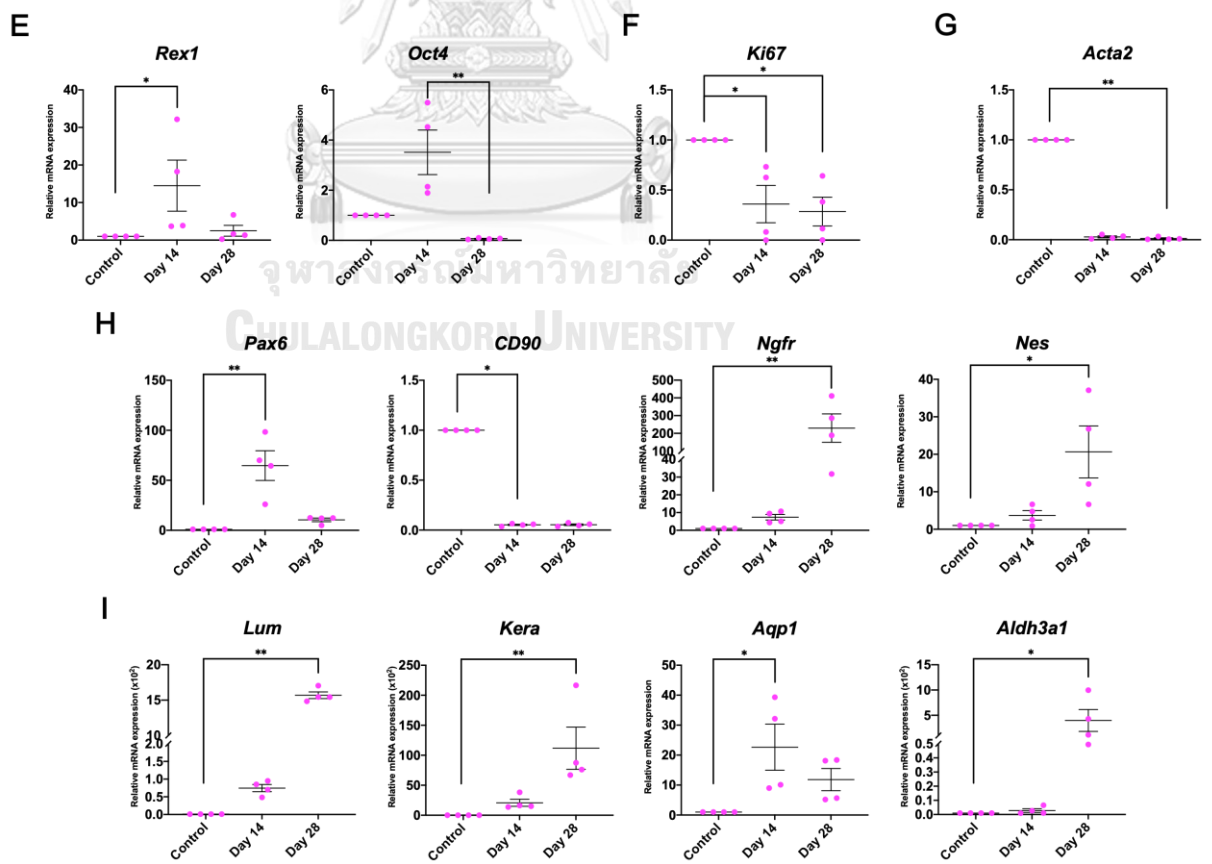


**Figure 7: mRNA expression of cLESCs seeded SF/G film and cSSCs seeded scaffold.**

Fold changes of RT-qPCR expression data of control (cells culture on tissue culture plate for 14 days), cLESCs seeded SF/G film at 14 and 28 days are presented. cLESCs seeded SF/G film at 14 and 28 days shows the upregulation of pluripotent (A), adult stemness-related markers (C) and epithelial cells markers (D) comparing to control. Proliferation marker shows upregulation at day 14 and downregulation at day 28 (B). RNA expression of pluripotent (E) and adult stemness-related markers (H) of cSSCs seeded SF/G scaffold reveals the upregulation at day 14, excepted CD90 shows downregulation at day 14 and 28. Proliferation marker (F) and myofibroblast marker (G) are downregulated at both time points. Upregulation at day 14 and 28 of both time points is presented by keratocyte marker (I). Values represent mean  $\pm$  SEM, n = 4 (\*p < 0.05, \*\*p<0.01).

Implemented SF/G films and scaffolds provided favorable biocompatibility

SEM imaged the morphology of cLESCs seeded film and cSSCs seeded scaffold from top view. cLESCs were feasibly adhered and aligned all over SF/G film area. Surface of cLESCs revealed polygonal cell shape and proximity to each other. 2-3 layers of stratified squamous epithelium were presented. The superficial cells exhibited bigger and less connection space of cell wall than basal cells. However, some cells were sloughed from the underlying layer (Figure 3A). SF/G scaffold comprehendingly provided cSSCs habitat. SEM detected cells overgrown onto and into the pores of sponge-like scaffold. The cells were spread out and distributed thorough the scaffold area. Fibrin-like extracellular matrix produced by cSSCs was observed on the surface and into the pores (Figure 3B).

Long term cell viability and distribution of cLESCs seeded SF/G film and cSSCs seeded scaffold were determined at day 1,3,5,7,14 and 28 and described by intracellular esterase activity and cell membrane permeability. Figure 3C and D appeared a large number of cells at all time points survived but a few dead cells indicated by green color at the cytoplasm and red nucleus respectively. cLESCs and cSSCs displayed plentiful distribution on SF/G films and SF/G scaffold at all time points respectively.

DNA measurement defined as cell proliferation assay was investigated using Qubit Flex Fluorometer. The dot plot graphs of DNA quantitation of cLESCs seeded SF/G film and cSSCs seeded SF/G scaffold were indicated cell proliferation at day 1, day 3, day 5, day7, day14 and day28. cLESCs seeded SF/G film increased proliferation at day1, day 3 and day 5 and rather unchanged among day 5, day 7, day 14 and day 28. Summarized data determined significant difference between day 1 and day 28 ( $p<0.05$ ) (Figure 3E). In cSSCs seeded SF/G scaffold, stable proliferation rate was manifested at day 1, day 3, day 5 and day 7 and obviously increased at day 14 and day 28. DNA levels were significantly different between day 5 and day 28 ( $p<0.05$ ) and day 7 and day 28 ( $p<0.05$ ) (Figure 3F).

In respect of gene expression, mRNA level was analyzed by RT-qPCR and presented by dot plot graph among day 14 of cell seeded on tissue culture plates (TCP, control), day 14 and day 28 of cells seeded on their own materials. Data of day 14 and day 28 were normalized by control. For cLESCs seeded SF/G film, stemness-related markers (*Rex1* and *Oct4*) revealed higher gene expression than control. *Rex1* at day 14 was significantly increased ( $p<0.05$ ), but no significant increase was presented at day 28 comparing to control (Figure 4A). *Oct4* was significantly increased from control to day 28 ( $p<0.05$ ). However, no significant increase was detected between control and day 14 (Figure 4A). Proliferation marker, *Ki67*, at day 14 was notably higher than control but significantly lower from day 14 to day 28 ( $p<0.01$ ) (Figure 4B). For the limbal stem cell markers (*Abcg2* and *P63*), levels of gene expression at day 14 and day 28 were higher than control. Significant upregulations appeared between control and day 14 of *Abcg2* ( $p<0.01$ ) (Figure 4C). *Krt3* and *Krt12*, epithelial cell marker, were increased by time. *Krt3* upregulation was significant at day 28 of ( $p<0.05$ ) (Figure 4D).

Apart from cLESCs seeded SF/G films, cSSCs seeded SF/G scaffold displayed upregulation of stemness-related markers (*Rex 1* and *Oct4*) at day 14 but downregulation at day 28. Significant difference was detected between control and day 14 ( $p < 0.05$ ) and day 14 and day 28 ( $p < 0.01$ ) of *Rex 1* and *Oct4* respectively (Figure 4E). For proliferation marker (*Ki67*) at day 14 and day 28 demonstrated downregulation comparing to control significantly ( $p < 0.05$ ) (Figure 4F). *Pax6* (stemness marker for corneal stromal cell) was similar pattern to stemness-related markers with significant increase at day 14 ( $p < 0.01$ ) (Figure 4H). Downregulation of *CD90* was illustrated both day 14 and day 28 ( $p < 0.05$ ). *Nes* and *Ngfr*, the neural crest gene associated with corneal stromal stem cell markers in human, were upregulated by time and significantly different at day 28 (Figure 4H). Myofibroblast marker was significantly downregulation both time points and significantly different at day 28 ( $p < 0.01$ ) (Figure 4G). Keratocyte specific gene markers (*Aldh3a1*, *Aqp1*, *Kera* and *Lum*) of day 14 and day 28 were higher than control, especially gene-related corneal ECM production (*Kera*, and *Lum*). More than 1000-fold elevation was presented at day 28 ( $p < 0.01$ ) (Figure 4I). *Aqp1* level was significantly higher at 14 ( $p < 0.05$ ) but not significantly decreased from day 14 to day 28. Significant upregulation was illustrated at day 28 of *Aldh3A1* ( $p < 0.05$ ) (Figure 4I). SF/G films and scaffolds provided as the acceptable cLESCs and cSSCs substrates for cell viability, cell proliferation, limbal epithelial stemness gene expression and differentiation of cSSCs into keratocytes.

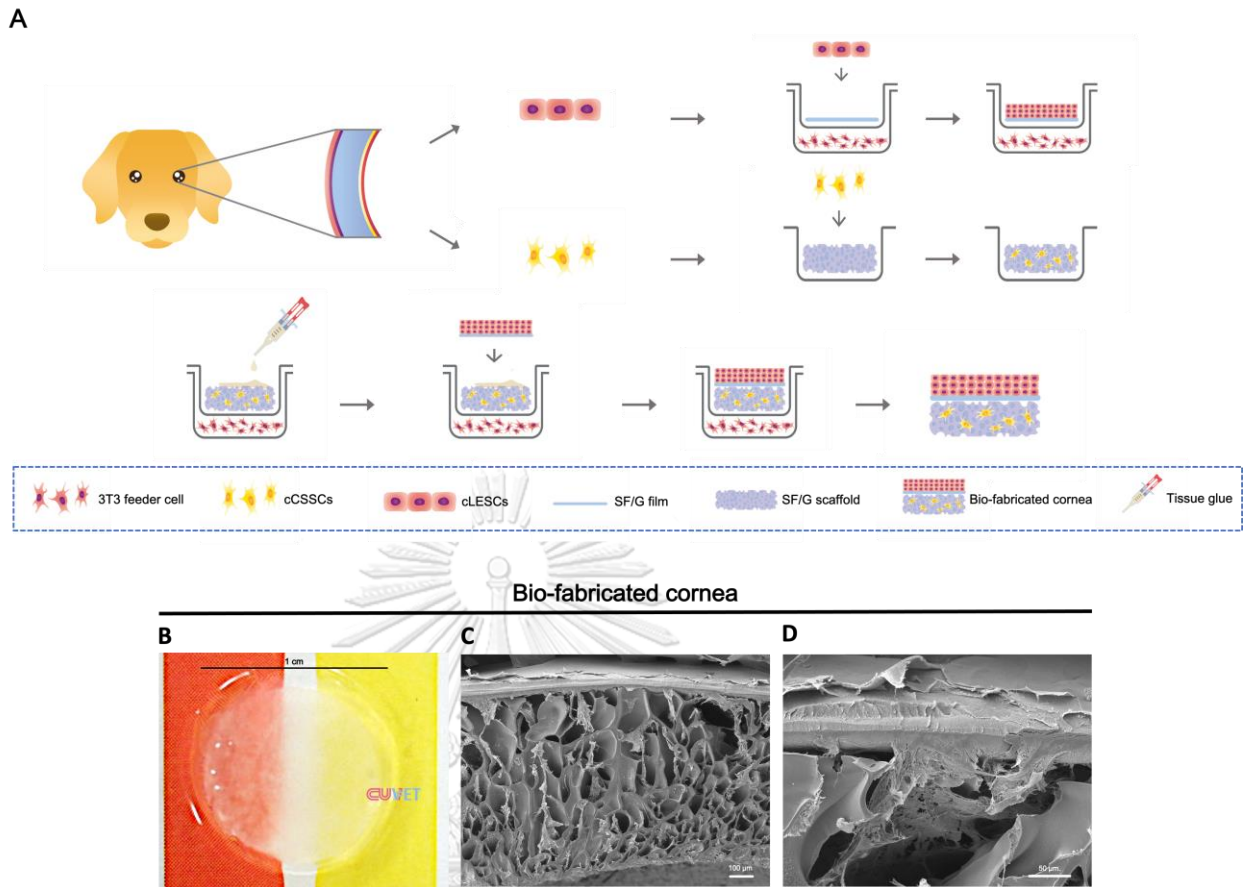


**Figure 8: Bio-fabricated cornea.**

Schematic illustration of the process to generate bio-fabricated cornea by assembling of cLESCs seeded SF/G film and cCSSCs seeded scaffold (A). Gross appearance of bio-fabricated cornea (B). SEM shows the upper layer of cLESCs seeded SF/G film align on the cCSSCs seeded SF/G scaffold (100x (C) and 350x (D))



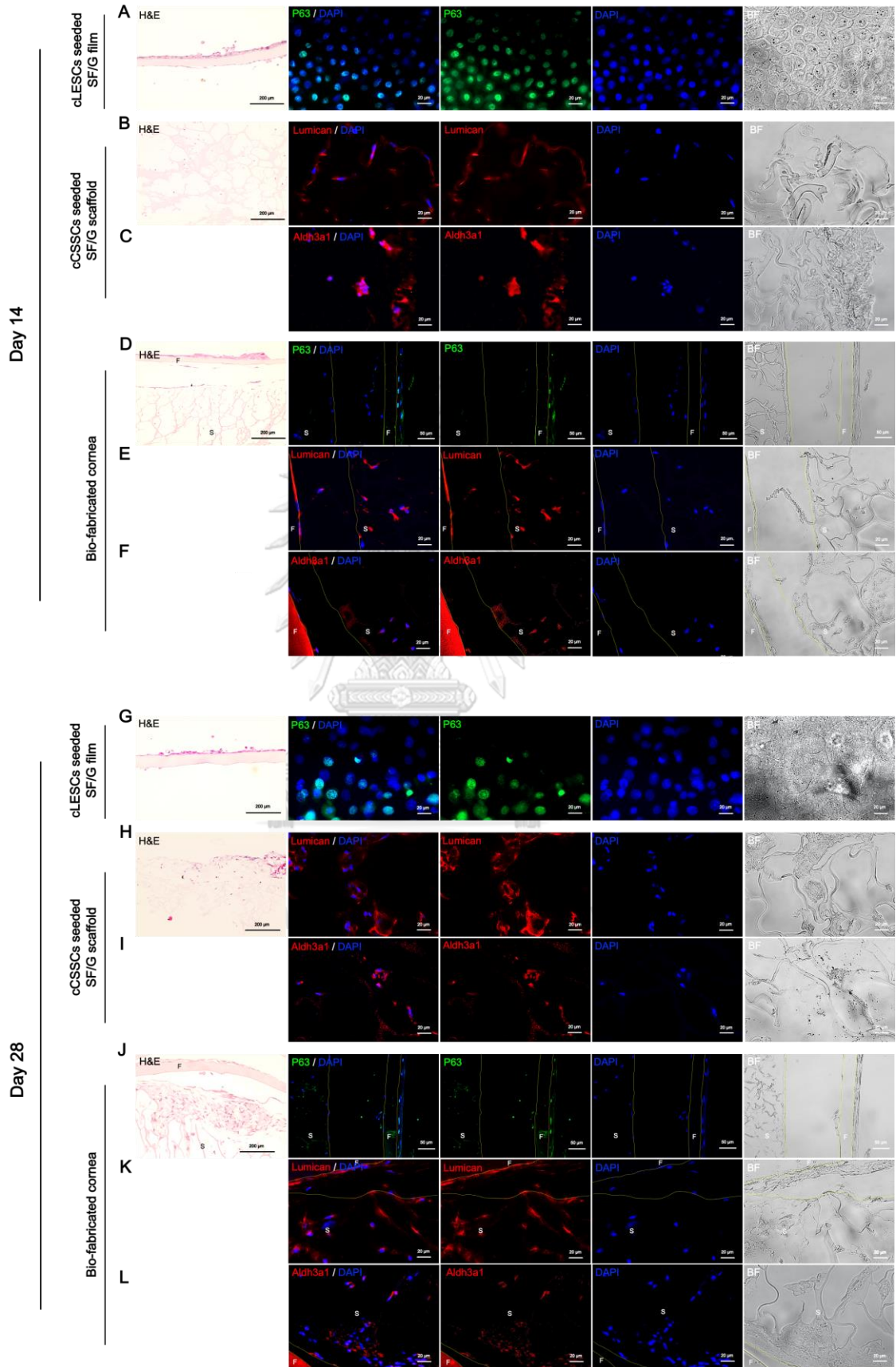


**Figure 9: Morphology and immunocytochemical profiles.**

H&E staining shows 2-3 layers of cLESCs upon SF/G film at day 14 (A) and day 28 (G) and upper part of bio-fabricated cornea at day 14 (D) and day 28 (J). cCSSCs distribute over SF/G scaffold at day 14 (B) and day 28 (H) and lower part of bio-fabricated cornea at day 14 (D) and day 28 (J). cLESCs seeded SF/G film at day 14 (A) shows more P63 positive nuclear staining cells than day 28 (G). P63 positive nuclear staining cells are detected at the basal cells of the upper part of bio-fabricated cornea at day 14 (D) and day 28 (J). Lumican positive cytoplasmic staining shows stronger intensity at day 28 of cCSSCs seeded SF/G scaffold (H) and lower part of bio-fabricated cornea (K) more than day 28 of cCSSCs seeded SF/G scaffold (B) and lower part of bio-fabricated cornea (E). Cytoplasmic staining of Aldh3a1 is similarly detected at day 14 and 28 of cCSSCs seeded SF/G scaffold (C, I) and bio-fabricated cornea (F, L) respectively. H&E figures image with 200x magnification. Immunofluorescences image with 400x magnification of all figures, except the figures of P63 of bio-fabricated cornea image with 200x. F, S are indicated to the area of SF/G film and SF/G scaffold respectively.

**Bio-fabricated corneal equivalents**

cLESCs seeded SF/G film and cCSSCs seeded SF/G scaffold were assembled to imitate natural cornea. cCSSCs seeded SF/G scaffold, acted as a corneal stroma, was covered by a synthetic corneal epithelium using cLESCs seeded SF/G film with tissue glue (Tisseel®; Baxter Corporation, USA). The procedure was presented by the infographic (Figure 5A).

After assembling, bio-fabricated cornea revealed 1-cm diameter of coin-like structure. The opacity was slightly increased comparing to cLESCs seeded SF/G film and cCSSCs seeded SF/G scaffold, nevertheless background paper color was visible. cLESCs seeded SF/G film was completely overlaid on cCSSCs seeded SF/G scaffold without detachment (Figure 5B).

To determine bio-fabricated cornea, SEM was executed to illustrate the integrated bio-materials at day 14 after co-culture. Cross-sectional figure demonstrated



the upper part of cLESCs seeded SF/G film adhered to the lower part of cCSSCs seeded SF/G scaffold, besides the interconnected space was absent. SF/G films maintained a stable structure and smooth substrate for cLESCs. Flat squamous cLESCs were contentedly aligned on the SF/G film, approximately 2-3 layers (Figure 5C). In addition, SF/G scaffolds were able to sustain their construction according to no evidence of collapsed pores. cCSSCs were infiltrated and dispersed into the sponge-like scaffold pores. Cell attachment was observed within each pore as well as come across to the pore nearby (Figure 5C). Interestingly, interconnected space was incorporated by tissue glue residual and ECM production (Figure 5D).

Histology and immunohistochemistry were performed at day 14 and 28 of cLESCs seeded SF/G film, cCSSCs seeded SF/G scaffold and bio-fabricated cornea to evaluate P63 (cLESCs marker), lumican (ECM of differentiated keratocyte) and Aldh3a1 (marker of differentiated keratocyte). H&E investigated 2-3 layers of stratified cLESCs cultivated on day 14 and 28 of SF/G films and bio-fabricated cornea. From top view of cLESCs seeded SF/G films, a large number of P63 represented cells were abundant and strongly presented at day 14 (Figure 6A), but rather decreased at day 28 (Figure 6G). Moreover, cross sectional bio-fabricated cornea detected P63 presented cells, particularly at the basal layer at both time points (Figure 6D, J). cCSSCs distribution and adherence along the surface of sponge-like scaffold pores were also investigated by H&E (Figure 6B,F,H). Besides, bio-fabricated cornea manifested the two bio-material integration mimicked natural cornea defined as the upper part of corneal epithelium and the lower part of corneal stroma (Figure 6D, J). At day 14 and 28 of cCSSCs seeded SF/G scaffold and bio-fabricated cornea showed fluorescent imaging of lumican and Aldh3a1 deposited by keratocyte differentiated cells (Figure 6B, C, E, F, H, I, K and L). Comparing between 2 time points, expression of lumican generated by keratocyte differentiated cells at day 28 was more robust and plentiful than day 14, on the other hand Aldh3a1 expression at day 28 was alike (Figure 6B,C,E,F,H,I,K and L).

For collagen type I (Col-1), abundant in corneal stroma, was analyzed by immunohistochemical examination. cSSCs seeded SF/G scaffold revealed collagen type I fibrils deposited by keratocyte differentiated cells (Figure 7A, B). Likewise, the expression at day 14 and day 28 was difficult to make the comparison described by the semi-quantitative analysis of color intensity. The adherence cells, stood by the surface of the pore, generated the collagen fibrils aligned along the surface of scaffold (Figure 7A), in contrast the cells that stayed inside the pore with no scaffold adherence, showed less potential to unidirectional alignment (Figure 7B). Lasting, bio-fabricated corneal equivalents were capable to imitate bona fide cornea in the part of epithelial and stomal layers.

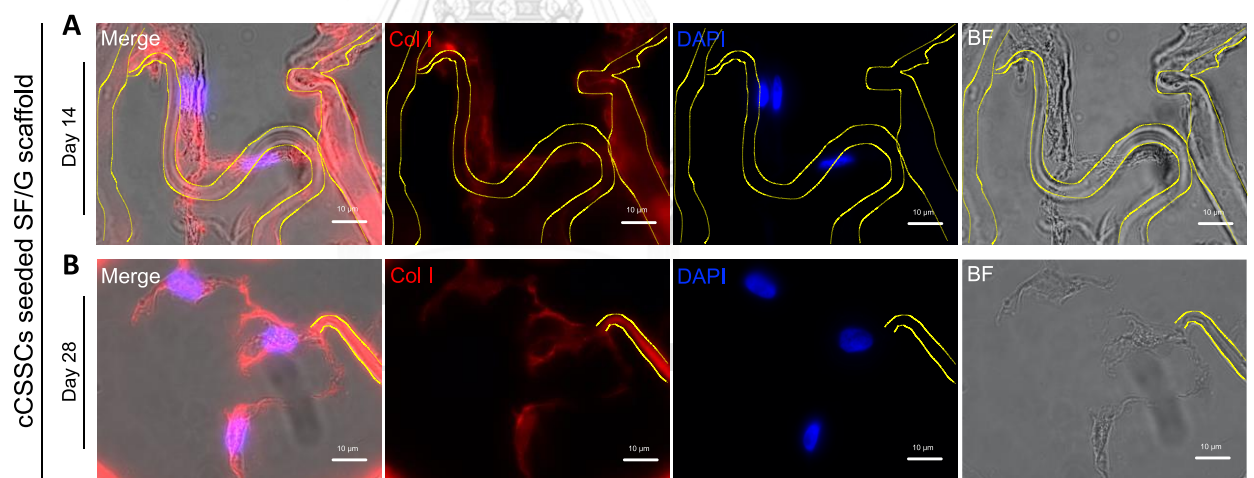


**Figure 10: Immunofluorescent staining of Collagen I.**

Keratocyte differentiated cells express collagen I at extracellular compartment at day 14 (A) and day 28 (B). Immunofluorescences image with 1000x magnification. Scaffolds are maginated by yellow border.

## Discussion

A stem cell niche for corneal limbal epithelial stem cells (LESCs), is verified by located in limbal area, called corneoscleral junction. Corneal epithelial stem cells play an important role for self-renewal and corneal epithelial wound healing (Secker and Daniels, 2009) The enzymatic isolation method of LESCs ordinarily accomplished with dispase and trypsin (Koizumi et al., 2002). However, nowadays, collagenase isolation provides superior efficiency because of the capacity to remove more basal epithelial progenitor cells, close-proximity mesenchymal cells and maintain some basement membrane matrix. Herein, this study firstly determined the potential of collagenase isolation in canine LESCs described by holoclones formation within 3 days and expression of stemness-related markers (*Rex 1* and *Oct4*), proliferation marker (*Ki67*), limbal stem cell markers (*Abcg2* and *P63*) and corneal epithelial markers (*Krt3* and *Krt12*). The expression of the limbal stem cell marker (*Abcg2* and *P63*) and corneal epithelial markers (*Krt3* and *Krt12*) showed heterogeneous population, mixed between limbal stem cells, progenitor cell and epithelial cells. However, *P63 $\alpha$* , widely recognized as a limbal stem cell marker in human and canine, was illustrated the majority of positive cell staining from the aforementioned immunocytochemistry result (Di Iorio et al., 2005; Nam et al., 2015). Recently, the hypothesis of LESCs supported by adjacent stromal microenvironment and corneal stromal stem cells (CSSCs) in 3-D structure is proved in term of promoting cell proliferation, colony formation and limbal stem cell gene expression (Nakatsu et al., 2014). Apart from hCSSCs (human corneal stromal stem cells), cCSCs (canine corneal stromal cells) also described as a multipotent mesenchymal stem cells which possess stem cell marker expression (CD90, CD73, CD105, N-cadherin, and Pax6), trilineage differentiation and innate immune privilege (Kafarnik et al., 2020). The expression of adult and pluripotent stemness-related markers (*Rex 1*, *Oct4*, *Pax6*, *Ngfr*, *Nes* and *CD90*) in this study was fulfilled stem cell-based knowledge of cell-derived canine corneal stromal stem cells. Transcription factor Pax6 (oculorhombin), important for ocular development, was

discovered in many embryonic ocular tissues, except keratocytes, and detected to be the marker of limbal stromal stem cell with nuclear immunostaining (Funderburgh et al., 2005). Unlike canine cells, human limbal niche cells manifested Pax6 positive nuclear staining but negative exhibition in nucleus of central stromal cells while this expression was detected at both positions in canine corneal stromal cell as well as positive nuclear staining of cSSCs in this study (Kafarnik et al., 2020). Moreover, Pax6 was investigated to play a crucial role for self-renewal capacity and sustain holoclone formation of limbal epithelial cells (Chen et al., 2019).

Since canine cornea donors and grafts are not only inadequate but also have some limitation, bioengineered canine cornea has been a fascinating alternative for a promising corneal graft. To develop corneal implantable bioequivalents in this study aims to mimic epithelium and stromal layers which are commonly problematic in clinical disease. As the result, SF/G was successfully fabricated to smooth surface film acted as a basement membrane of epithelial layer and sponge-like scaffold processed abundant ECM component lattice served for corneal stroma.  $130.71 \pm 37.12 \mu\text{m}$  pore size was created using freeze-dry method which is consistent with the range of 95.9–150.5  $\mu\text{m}$  that promoted cell attachment and viability (O'Brien et al., 2005). Corneal transparency and structure maintenance are correlated with suitable water content. The results of water content from SF/G film and SF/G scaffold indicated this 75-90% range at all time points, close to normal human cornea (Taylor et al., 2015). Nevertheless, SF/G film showed slightly decreased % water content due to water solubility. This phenomenon might possibly be caused by the large amount of non-crosslink gelatin (70%) and inadequate  $\beta$ -sheet formation from water annealing at 25 °C. Hence, the higher temperature at 95 °C performed  $\beta$ -sheet up to 60% might be suggested for the future experiments. (Hu et al., 2011). Degradation rate was evaluated by protease XIV solution as a result of the most efficient enzymatic degradation comparing to collagenase IA and  $\alpha$ -chymotrypsin in silk protein (Li et al., 2003). SF/G scaffold presented faster shapeless and degradation rate than SF/G film, the

mentioned result interested in the porosity of scaffold investigated to be more vulnerable and faster degradation rate (Cunha-Reis et al., 2007; Gil et al., 2010b; Higa et al., 2011; Suzuki et al., 2015). In the aspect of mechanical property, elastic moduli of both distinct materials were analyzed from different range of force, thus they were not comparable. However, their elastic moduli were in range of natural human cornea (0.3-7Mpa) (Bakhshandeh et al., 2011). In addition, elastic modulus and UTS of SF/G film detected higher owing to absence of porosity, likewise the aforementioned result (Gil et al., 2010b; Higa et al., 2011; Suzuki et al., 2015).

Interestingly, Wu et al. 2014 revealed the crucial rule of RGD, arginine-glycine-aspartic acid for integrin related cell attachment, especially in hCSCs (Wu et al., 2014b) (Wu et al., 2014b). SF itself shows a lack of RGD sequence, mixing with RGD motif contained gelatin can promote cell adhesion capacity with unnecessary RGD-modified process. The results of figure 3A-D firstly illustrated cell adhesion capacity and cell viability up to 28 days of SF/G materials with canine corneal cells. The proliferation of cLESCs seeded SF/G film exhibited proliferative phase after day 3 following with plateau phase after day 5. Similar to hLESCs seeded collagen I substrate, the pattern of growth curve showed proliferative phase between 3 days and 7 days (Forni et al., 2013). The mentioned result implies that SF/G and collagen I were comparable materials for LESC in term of promoting cell proliferation. While the proliferation rate of cCSCs manifested plateau phase up to 7 days then following with log phase. This scenario can be interpreted as the effect of serum free media, KDM, associated with slow cell growth (Liu et al., 2011). In contrast, Foster et al., revealed the growth rate of human corneal stromal cells in serum free media with low glucose after 3 days and remained plateau after 7 days, however this study underwent in 2-d condition (Foster et al., 2015).

For cLESCs seeded SF/G film, the expression of pluripotent (*Rex 1 and Oct4*) and adult stemness-related markers, *Abcg2* at day 14 and *P63* at day 14 and 28 were higher than those cultured in TCP. This phenomenon might be affected by suitable

matrix stiffness of SF/G to cLESCs behavior as well as the study of Gouveia et al. exhibited the relation between soft substrates and LESC marker. The result showed the superior efficiency to maintain ABCG2 and P63 in soft substrate via mechanotransduction (Gouveia et al., 2019).

However, the proliferation marker (*Ki67*) at day 28 was significant lower. This result was correlated with proliferation assay that exhibited slow proliferation at late period which was possibly caused by contact inhibition (McClatchey and Yap, 2012). Morita et al. and Nam et al. indicated ABCG2 and P63 as a marker of limbal corneal epithelial stem cells (LESCs) and corneal epithelial cell proliferation respectively, therefore to utilize those makers in this study was validated (Morita et al., 2015; Nam et al., 2015). P63 can detect both TACs (transient amplifying cells) and stem cells whereas ABCG2 detects only stem cells, this fact suggested that, from day 14 to day 28, SF/G film could enhance the differentiation property from stem cells to TACs and finally to terminal differentiated cells (corneal epithelial cells) defined as greater expression of *Krt3* and *Krt12* (Philp et al., 2005). However, stem cell population was still preserved heterogenous population similar to native cornea.

Pluripotent and adult stemness markers (*Rex 1*, *Oct4*, *Pax6*, *Ngfr*, *Nes*) of cSSCs seeded SF/G scaffold at day 14 were upregulated compared to cell seeded in TCP, although culturing system was exposed to KDM. Consequently, these outstanding results pointed to stemness preserved ability of cell seeded scaffold as well as the result of mesenchymal stem cell (MSC) from juvenile bovine bone marrow that maintains stemness markers in Poly ( $\epsilon$ -caprolactone) (PCL) nanofibrous scaffolds than TCP (Heo et al., 2018). In contrast, the adverse results of pluripotent and adult stemness markers (*Rex 1*, *Oct4*, *Pax6*) at day 28 alluded to long term culture and potential of KDM to differentiated keratocytes. In addition, those mentioned juvenile bovine MSC also explained the lower expression of *Ki67* (proliferation marker) in this study comparing to TCP since MSCs are activated toward a fibrotic differentiation pathway, regulated by increase MSC contractility and YAP activation resulting in

increase of cell proliferation (Heo et al., 2018). Arise from cell differentiation, *CD90* (well-accepted MSC marker) was downregulated at day 14 and day 28 compared to TCP. As a consequence of *CD90* investigation in fibroblast, cSSCs seeded scaffold was commendable in term of avoiding fibroblast and myofibroblast, described by downregulation of *CD90 and ACTA2* (Dominici et al., 2006). The aforementioned results supported the advantage of those bio-fabricated corneal equivalents considering fibroblast and myofibroblast are responsible to generate unorganized stromal ECM, resulting in opaque corneal scar formation (Wilson et al., 2001). In addition, *KERA* and *LUM*, ECM molecules associated with spacing and collagen fibril organization related to corneal transparency, were significantly upregulated at day 28. The achievement of keratocyte differentiation was marvelously encouraged by stellate typical keratocyte morphology, the expression of ECM-related keratocyte gene (*Lum, Kera*) and the expression of keratocyte specific markers (*Aqp1, Aldh3a1*,). Surprisingly, aquaporin-1 (*Aqp1*) water channels, are presented in human corneal keratocytes associated with cell migration and corneal wounding, was firstly discovered in canine keratocyte differentiated cells (Ruiz-Ederra and Verkman, 2009). Besides, *ALDH3A1*, corneal crystallins, plays an essential rule to protect ocular tissue from ultraviolet radiation (UVR)-induced oxidative damage via non-catalytic and catalytic mechanisms (Estey et al., 2007). In human study, *AQP1 and ALDH3A1*, keratocyte markers, were upregulated within 21 days after differentiation, likewise this study, the expression of *Aqp1* and *Aldh3a1* were significantly upregulated at day 14 and 28 respectively (Basu et al., 2014; Du et al., 2005; Park et al., 2012). However, no significant downregulation from day 14 of *Aqp1* was observed on day 28 (Figure 4B).

Bio-fabricated cornea composed of cLESCs seeded SF/G upon cSSCs seeded SF/G scaffold connected by tissue glue sealant (Tisseel®; Baxter Corporation, USA). Figure 5B manifested structural stability corresponding to be manipulatable, transferable as well as suturable. Slightly hazy appearance of bio-fabricated cornea signified its limitation comparing to transparent corneal graft. Nevertheless, the

actuality of scaffold degradation is anticipated after *in vivo* transplantation and organized ECM by keratocyte differentiated cells are prospective to generate corneal transparency ultimately. Similarity to an auto-tissue-engineered lamellar cornea (ATELC), acellular porcine corneal stroma with autologous corneal limbal explants in rabbit model, showed desirable transparency 20 days after transplantation (Wu et al., 2014c). A fibrin sealant product, Tisseel (Tisseel®; Baxter Corporation), completely performed a fibrin polymerization to seal and stabilize between 2 materials. Fibrinogen, supplied by product, is converted to fibrin monomer and forms fibrin polymer which binds the separated tissue as well as hemostasis. Moreover, Tisseel (Tisseel®; Baxter Corporation) has been favored in several oculoplastics surgeries including sutureless lamellar keratoplasty, pterygium surgery, and management of bleb leaks in humans (Yeh and Tucker, 2005).

cLESCs seeded SF/G film, represented by successful adherence, proliferation and stratification of cLESCs upon SF/G. Air-liquid interface cell culture is rationally accepted to promote epithelial proliferation, differentiation and stratification affected by the shift of oxidative metabolism from the growth phase to the differentiation phase and contributes a polarization effect allowing proper stratification (Kondo et al., 1997; Zieske et al., 1994). Under air-liquid interface condition, H&E represented cell proliferation and 2-3 layers of stratification of cLESCs seeded SF/G film at day 14 and day 28 as well as bio-fabricated cornea at day 14 and day 28. According to logical postulate, cLESCs seeded SF/G film at day 28 obviously presented morphological feature of cell differentiation than day 14, characterized by large size, large nucleus and low nucleo-cytoplasmic ratio (Doughty, 2015). P63 expression from immunohistochemistry defined consistency of decrease P63 expression at day 28 by differentiated property, related to *Krt3* and *Krt 12* upregulation and *Abcg2* downregulation. Although *P63* revealed upregulation at day 14 and day 28, no significant difference was detected. Moreover, bio-fabricated cornea that was illustrated the cross-section of cLESCs seeded SF/G film at day 14 and 28 locally



detected strong positive P63 expression at basal layer, where corneal stem cells are located (Figure 6A, B).

cSSCs, distributed throughout SF/G scaffold and bio-fabricated cornea at day 14 and 28, exhibited Aldh3a1 and lumican expression which referred to the first achievement of canine keratocyte differentiation in SF/G scaffold. Lumican, a major keratan sulfate proteoglycan responding to corneal transparency, appeared stronger expression by culturing time related to *Lum* gene expression that upregulated over 1000 folds. Meanwhile, Aldh3a1 expression was detected but difficult to compare (Figure 6A, B).

Corneal stroma is abundant collagenous connective tissue, produced by keratocytes. Collagen is accountable for optical transparency, the refraction and mechanical strength. Collagen type-I (Col-1), collagen type-V (Col-V) and collagen type-VI (Col-VI) are considerably discovered in corneal stroma (Birk et al., 1986). In this study, col-1 expression of canine keratocyte differentiated cells was firstly investigated by immunohistochemistry. The positive result was impliedly stipulated by successful differentiation into keratocyte, proper scaffold and growth factors. Wu et al. explored the positive relation between collagen producing cells, human corneal stromal stem cells, with RGD-modify silk scaffold. With RGD coupling, collagen fibrils were robustly aligned and distributed (Wu et al., 2014b). Besides, FGF-2 and TGF- $\beta$ 3 favorably activated the production of a stromal-like tissue composed of multilayered lamellae with orthogonal oriented collagen fibrils and the cornea-specific proteins and proteoglycans (Wu et al., 2013). Figure 7A, B revealed col-1 expression in distinct alignment described by the position of collagen producing cells. The cells adhered proximity to scaffold exhibited the collagen alignment along the scaffold surface while the cell existed far away from scaffold generated non directional and scattered collagen alignment. As mentioned above signified that collagen can be manipulated its direction via the surface of scaffold. In term of multilayered lamellae with orthogonally oriented collagen fibrils in corneal stroma, topographical modification of

scaffold is beneficial to regulated collagen direction imitated in the healthy cornea. For example, groove topography successfully manifested well-defined lamella collagen orientation and promoted proper ECM including keratan sulfate, lumican, and keratocan (Ghezzi et al., 2017; Wu et al., 2014b)

Based on the aforementioned results provided the knowledge of cLESCs and cSSCs for corneal tissue engineering with SF/G based scaffold. SF/G would hypothetically be degraded after transplantation while cLESCs and keratocyte differentiated cells would be colonized and contributed essential ECM and collagen in native cornea. To modified topography supported multilayered collagen lamellae will be generated for canine corneal tissue construct in the future.



## CHAPTER 5

### CONCLUSION

SF/G film and SF/G scaffold were achieved to support cell adhesion, viability, proliferation as well as to maintain cLESCs and cSSCs differentiate into keratocytes. This study endeavored to generate biocompatible and transplantable canine corneal equivalents in part of the epithelial and stromal layer using cLESCs seeded SF/G films and cSSCs seeded SF/G scaffolds respectively. Collagen and endogenous ECM production exhibited the capability to imitate the native cornea after 14 days.



## REFERENCES



จุฬาลงกรณ์มหาวิทยาลัย  
**CHULALONGKORN UNIVERSITY**

Agarwal, N., Hoagland, D., Farris, R., 1997. Effect of moisture absorption on the thermal properties of Bombyx mori silk fibroin films. *Journal of Applied Polymer Science* 63, 401-410.

Almaliotis, D., Koliakos, G., Papakonstantinou, E., Komnenou, A., Thomas, A., Petrakis, S., Nakos, I., Gounari, E., Karampatakis, V., 2015. Mesenchymal stem cells improve healing of the cornea after alkali injury. *Graefe's Archive for Clinical and Experimental Ophthalmology* 253, 1121-1135.

Applegate, M.B., Partlow, B.P., Coburn, J., Marelli, B., Pirie, C., Pineda, R., Kaplan, D.L., Omenetto, F.G., 2016. Photocrosslinking of silk fibroin using riboflavin for ocular prostheses. *Advanced Materials* 28, 2417-2420.

Arcelli, R., Tibaldini, P., Angeli, G., Bellezza, E., 2009. Equine amniotic membrane transplantation in some ocular surface diseases in the dog and cat: a preliminary study. *Veterinary research communications* 33, 169-171.

Bakhshandeh, H., Soleimani, M., Hosseini, S.S., Hashemi, H., Shabani, I., Shafiee, A., Nejad, A.H.B., Erfan, M., Dinarvand, R., Atyabi, F., 2011. Poly ( $\epsilon$ -caprolactone) nanofibrous ring surrounding a polyvinyl alcohol hydrogel for the development of a biocompatible two-part artificial cornea. *International journal of nanomedicine* 6, 1509.

Barbaro, V., Testa, A., Di Iorio, E., Mavilio, F., Pellegrini, G., De Luca, M., 2007. C/EBP $\delta$  regulates cell cycle and self-renewal of human limbal stem cells. *The Journal of cell biology* 177, 1037-1049.

Barros, P.S., Garcia, J.A., Laus, J., Ferreira, A.L., Salles Gomes, T., 1998. The use of xenologous amniotic membrane to repair canine corneal perforation created by penetrating keratectomy. *Veterinary Ophthalmology* 1, 119-123.

Barros, P.S., Safatle, A.M., Godoy, C.A., Souza, M.S., Barros, L.F., Brooks, D.E., 2005. Amniotic membrane transplantation for the reconstruction of the ocular surface in three cases. *Veterinary Ophthalmology* 8, 189-192.

Basu, S., Hertszenberg, A.J., Funderburgh, M.L., Burrow, M.K., Mann, M.M., Du, Y., Lathrop, K.L., Syed-Picard, F.N., Adams, S.M., Birk, D.E., 2014. Human limbal biopsy-derived stromal stem cells prevent corneal scarring. *Science translational medicine* 6, 266ra172-266ra172.

- Bertoldi, M., 2016. Il sequestro corneale felino: tecniche chirurgiche, revisione della letteratura e studio retrospettivo della casistica clinica.
- Bhat, R., Karim, A., 2009. Ultraviolet irradiation improves gel strength of fish gelatin. *Food chemistry* 113, 1160-1164.
- Bigi, A., Cojazzi, G., Panzavolta, S., Roveri, N., Rubini, K., 2002. Stabilization of gelatin films by crosslinking with genipin. *Biomaterials* 23, 4827-4832.
- Birk, D., Fitch, J., Linsenmayer, T., 1986. Organization of collagen types I and V in the embryonic chicken cornea. *Investigative ophthalmology & visual science* 27, 1470-1477.
- Bourne, W.M., Nelson, L.R., Hodge, D.O., 1997. Central corneal endothelial cell changes over a ten-year period. *Investigative ophthalmology & visual science* 38, 779-782.
- Bray, L.J., George, K.A., Ainscough, S.L., Hutmacher, D.W., Chirila, T.V., Harkin, D.G., 2011. Human corneal epithelial equivalents constructed on Bombyx mori silk fibroin membranes. *Biomaterials* 32, 5086-5091.
- Bray, L.J., George, K.A., Hutmacher, D.W., Chirila, T.V., Harkin, D.G., 2012. A dual-layer silk fibroin scaffold for reconstructing the human corneal limbus. *Biomaterials* 33, 3529-3538.
- Brinkman, W.T., Nagapudi, K., Thomas, B.S., Chaikof, E.L., 2003. Photo-cross-linking of type I collagen gels in the presence of smooth muscle cells: mechanical properties, cell viability, and function. *Biomacromolecules* 4, 890-895.
- Brunelli, A., Vicente, F., Chahud, F., Oriá, A., Bolzan, A., Campos, C., Doria Neto, F., Laus, J., 2007. Sclerocorneal limbal stem cell autograft transplantation in dogs. *Arquivo Brasileiro de Medicina Veterinária e Zootecnia* 59, 1194-1204.
- Carlsson, D.J., Li, F., Shimmura, S., Griffith, M., 2003. Bioengineered corneas: how close are we? *Current opinion in ophthalmology* 14, 192-197.
- Chakravarti, S., Petroll, W.M., Hassell, J.R., Jester, J.V., Lass, J.H., Paul, J., Birk, D.E., 2000. Corneal opacity in lumican-null mice: defects in collagen fibril structure and packing in the posterior stroma. *Investigative ophthalmology & visual science* 41, 3365-3373.
- Chantong, N., Damrongsakkul, S., Ratanavaraporn, J., 2019. Gelation Process and Physicochemical Properties of Thai Silk Fibroin Hydrogels Induced by Various Anionic Surfactants for Controlled Release of Curcumin. *Journal of Surfactants and Detergents*.

- Chen, S., Mienaltowski, M.J., Birk, D.E., 2015. Regulation of corneal stroma extracellular matrix assembly. *Experimental eye research* 133, 69-80.
- Chen, S.-Y., Cheng, A.M., Zhang, Y., Zhu, Y.-T., He, H., Mahabole, M., Tseng, S.C., 2019. Pax 6 controls neural crest potential of limbal niche cells to support self-renewal of limbal epithelial stem cells. *Scientific reports* 9, 1-13.
- Chen, Z., de Paiva, C.S., Luo, L., Kretzer, F.L., Pflugfelder, S.C., Li, D.Q., 2004. Characterization of putative stem cell phenotype in human limbal epithelia. *Stem cells* 22, 355-366.
- Chen, Z., You, J., Liu, X., Cooper, S., Hodge, C., Sutton, G., Crook, J.M., Wallace, G.G., 2018. Biomaterials for corneal bioengineering. *Biomedical Materials* 13, 032002.
- Cheng, J., Zhai, H., Wang, J., Duan, H., Zhou, Q., 2017. Long-term outcome of allogeneic cultivated limbal epithelial transplantation for symblepharon caused by severe ocular burns. *BMC ophthalmology* 17, 8.
- Cotsarelis, G., Cheng, S.-Z., Dong, G., Sun, T.-T., Lavker, R.M., 1989. Existence of slow-cycling limbal epithelial basal cells that can be preferentially stimulated to proliferate: implications on epithelial stem cells. *Cell* 57, 201-209.
- Cunha-Reis, C., Tuzlakoglu, K., Baas, E., Yang, Y., El Haj, A., Reis, R., 2007. Influence of porosity and fibre diameter on the degradation of chitosan fibre-mesh scaffolds and cell adhesion. *Journal of Materials Science: Materials in Medicine* 18, 195-200.
- Cursiefen, C., Chen, L., Dana, M.R., Streilein, J.W., 2003. Corneal lymphangiogenesis: evidence, mechanisms, and implications for corneal transplant immunology. *Cornea* 22, 273-281.
- Daya, S.M., Watson, A., Sharpe, J.R., Giledi, O., Rowe, A., Martin, R., James, S.E., 2005. Outcomes and DNA analysis of ex vivo expanded stem cell allograft for ocular surface reconstruction. *Ophthalmology* 112, 470-477.
- de Araujo, A.L., Gomes, J.Á.P., 2015. Corneal stem cells and tissue engineering: Current advances and future perspectives. *World journal of stem cells* 7, 806.
- DelMonte, D.W., Kim, T., 2011. Anatomy and physiology of the cornea. *Journal of Cataract & Refractive Surgery* 37, 588-598.
- Demirayak, B., Yüksel, N., Çelik, O.S., Subaşı, C., Duruksu, G., Unal, Z.S., Yıldız, D.K., Karaöz, E., 2016. Effect of bone marrow and adipose tissue-derived mesenchymal stem

cells on the natural course of corneal scarring after penetrating injury. *Experimental eye research* 151, 227-235.

Di Iorio, E., Barbaro, V., Ruzza, A., Ponzin, D., Pellegrini, G., De Luca, M., 2005. Isoforms of  $\Delta$ Np63 and the migration of ocular limbal cells in human corneal regeneration. *Proceedings of the National Academy of Sciences* 102, 9523-9528.

Dohlman, C.H., 1971. The function of the corneal epithelium in health and disease. *Invest Ophthalmol* 10, 381-407.

Dominici, M., Le Blanc, K., Mueller, I., Slaper-Cortenbach, I., Marini, F., Krause, D., Deans, R., Keating, A., Prockop, D., Horwitz, E., 2006. Minimal criteria for defining multipotent mesenchymal stromal cells. The International Society for Cellular Therapy position statement. *Cytotherapy* 8, 315-317.

Dong, Y., Peng, H., Lavker, R.M., 2018. Emerging therapeutic strategies for limbal stem cell deficiency. *Journal of ophthalmology* 2018.

Doughty, M.J., 2015. Assessment of size and nucleo-cytoplasmic characteristics of the squamous cells of the corneal epithelium. *Clinical and Experimental Optometry* 98, 218-223.

Du, Y., Carlson, E.C., Funderburgh, M.L., Birk, D.E., Pearlman, E., Guo, N., Kao, W.W.Y., Funderburgh, J.L., 2009. Stem cell therapy restores transparency to defective murine corneas. *Stem cells* 27, 1635-1642.

Du, Y., Funderburgh, M.L., Mann, M.M., SundarRaj, N., Funderburgh, J.L., 2005. Multipotent stem cells in human corneal stroma. *Stem cells* 23, 1266-1275.

Dua, H.S., Azuara-Blanco, A., 2000. Limbal stem cells of the corneal epithelium. *Survey of ophthalmology* 44, 415-425.

Dziasko, M.A., Armer, H.E., Levis, H.J., Shortt, A.J., Tuft, S., Daniels, J.T., 2014. Localisation of epithelial cells capable of holoclone formation in vitro and direct interaction with stromal cells in the native human limbal crypt. *PloS one* 9, e94283.

Dziasko, M.A., Daniels, J.T., 2016. Anatomical features and cell-cell interactions in the human limbal epithelial stem cell niche. *The ocular surface* 14, 322-330.



- Dziasko, M.A., Tuft, S.J., Daniels, J.T., 2015. Limbal melanocytes support limbal epithelial stem cells in 2D and 3D microenvironments. *Experimental eye research* 138, 70-79.
- Estey, T., Piatigorsky, J., Lassen, N., Vasiliou, V., 2007. ALDH3A1: a corneal crystallin with diverse functions. *Experimental eye research* 84, 3-12.
- Fan, H., Liu, H., Toh, S.L., Goh, J.C., 2008. Enhanced differentiation of mesenchymal stem cells co-cultured with ligament fibroblasts on gelatin/silk fibroin hybrid scaffold. *Biomaterials* 29, 1017-1027.
- Forni, M.F., Loureiro, R.R., Cristovam, P.C., Bonatti, J.A., Sogayar, M.C., Gomes, J.Á.P., 2013. Comparison between different biomaterial scaffolds for limbal-derived stem cells growth and enrichment. *Current eye research* 38, 27-34.
- Foster, J.W., Gouveia, R.M., Connon, C.J., 2015. Low-glucose enhances keratocyte-characteristic phenotype from corneal stromal cells in serum-free conditions. *Scientific reports* 5, 1-16.
- Funderburgh, J.L., Funderburgh, M.L., Du, Y., 2016. Stem cells in the limbal stroma. *The ocular surface* 14, 113-120.
- Funderburgh, J.L., Mann, M.M., Funderburgh, M.L., 2003. Keratocyte phenotype mediates proteoglycan structure a role for fibroblasts in corneal fibrosis. *Journal of Biological Chemistry* 278, 45629-45637.
- Funderburgh, M.L., Du, Y., Mann, M.M., SundarRaj, N., Funderburgh, J.L., 2005. PAX6 expression identifies progenitor cells for corneal keratocytes. *The FASEB journal* 19, 1371-1373.
- Gao, Y., Yan, J., Cui, X., Wang, H., Wang, Q., 2012. Aligned fibrous scaffold induced aligned growth of corneal stroma cells in vitro culture. *Chem. Res. Chin. Univ* 28, 1022-1025.
- Ghezzi, C.E., Marelli, B., Omenetto, F.G., Funderburgh, J.L., Kaplan, D.L., 2017. 3D functional corneal stromal tissue equivalent based on corneal stromal stem cells and multi-layered silk film architecture. *PloS one* 12, e0169504.
- Ghezzi, C.E., Rnjak-Kovacina, J., Kaplan, D.L., 2015. Corneal tissue engineering: recent advances and future perspectives. *Tissue Engineering Part B: Reviews* 21, 278-287.

- Gil, E.S., Mandal, B.B., Park, S.-H., Marchant, J.K., Omenetto, F.G., Kaplan, D.L., 2010a. Helicoidal multi-lamellar features of RGD-functionalized silk biomaterials for corneal tissue engineering. *Biomaterials* 31, 8953-8963.
- Gil, E.S., Park, S.H., Marchant, J., Omenetto, F., Kaplan, D.L., 2010b. Response of human corneal fibroblasts on silk film surface patterns. *Macromolecular bioscience* 10, 664-673.
- Gilger, B.C., Whitley, R., McLaughlin, S., Wright, J., Drane, J., 1991. Canine corneal thickness measured by ultrasonic pachymetry. *American journal of veterinary research* 52, 1570-1572.
- Gosselin, E.A., Torregrosa, T., Ghezzi, C.E., Mendelsohn, A.C., Gomes, R., Funderburgh, J.L., Kaplan, D.L., 2018. Multi-layered silk film coculture system for human corneal epithelial and stromal stem cells. *Journal of tissue engineering and regenerative medicine* 12, 285-295.
- Gouveia, R.M., Vajda, F., Wibowo, J.A., Figueiredo, F., Connon, C.J., 2019. YAP,  $\Delta$ Np63, and  $\beta$ -catenin signaling pathways are involved in the modulation of corneal epithelial stem cell phenotype induced by substrate stiffness. *Cells* 8, 347.
- Gupta, M.K., Khokhar, S.K., Phillips, D.M., Sowards, L.A., Drummy, L.F., Kadakia, M.P., Naik, R.R., 2007. Patterned silk films cast from ionic liquid solubilized fibroin as scaffolds for cell growth. *Langmuir* 23, 1315-1319.
- Hazra, S., Nandi, S., Naskar, D., Guha, R., Chowdhury, S., Pradhan, N., Kundu, S.C., Konar, A., 2016. Non-mulberry silk fibroin biomaterial for corneal regeneration. *Scientific reports* 6, 21840.
- Helper, L.C., 1989. *Magrane's canine ophthalmology*.
- Heo, S.J., Szczesny, S.E., Kim, D.H., Saleh, K.S., Mauck, R.L., 2018. Expansion of mesenchymal stem cells on electrospun scaffolds maintains stemness, mechano-responsivity, and differentiation potential. *Journal of Orthopaedic Research* 36, 808-815.
- Hertsenberg, A.J., Shojaati, G., Funderburgh, M.L., Mann, M.M., Du, Y., Funderburgh, J.L., 2017. Corneal stromal stem cells reduce corneal scarring by mediating neutrophil infiltration after wounding. *PloS one* 12, e0171712.

- Higa, K., Takeshima, N., Moro, F., Kawakita, T., Kawashima, M., Demura, M., Shimazaki, J., Asakura, T., Tsubota, K., Shimmura, S., 2011. Porous silk fibroin film as a transparent carrier for cultivated corneal epithelial sheets. *Journal of Biomaterials Science, Polymer Edition* 22, 2261-2276.
- Horan, R.L., Antle, K., Collette, A.L., Wang, Y., Huang, J., Moreau, J.E., Volloch, V., Kaplan, D.L., Altman, G.H., 2005. In vitro degradation of silk fibroin. *Biomaterials* 26, 3385-3393.
- Hu, X., Shmelev, K., Sun, L., Gil, E.-S., Park, S.-H., Cebe, P., Kaplan, D.L., 2011. Regulation of silk material structure by temperature-controlled water vapor annealing. *Biomacromolecules* 12, 1686-1696.
- Huang, M., Wang, B., Wan, P., Liang, X., Wang, X., Liu, Y., Zhou, Q., Wang, Z., 2015. Roles of limbal microvascular net and limbal stroma in regulating maintenance of limbal epithelial stem cells. *Cell and tissue research* 359, 547-563.
- Jester, J.V., Ho-Chang, J., 2003. Modulation of cultured corneal keratocyte phenotype by growth factors/cytokines control in vitro contractility and extracellular matrix contraction. *Experimental eye research* 77, 581-592.
- Jiang, Z., Liu, G., Meng, F., Wang, W., Hao, P., Xiang, Y., Wang, Y., Han, R., Li, F., Wang, L., 2017. Paracrine effects of mesenchymal stem cells on the activation of keratocytes. *British Journal of Ophthalmology* 101, 1583-1590.
- Jin, H.-J., Park, J., Valluzzi, R., Cebe, P., Kaplan, D.L., 2004. Biomaterial films of Bombyx Mori silk Fibroin with Poly (ethylene oxide). *Biomacromolecules* 5, 711-717.
- Jin, H.J., Park, J., Karageorgiou, V., Kim, U.J., Valluzzi, R., Cebe, P., Kaplan, D.L., 2005. Water-stable silk films with reduced  $\beta$ -sheet content. *Advanced Functional Materials* 15, 1241-1247.
- Joyce, N.C., 2005. Cell cycle status in human corneal endothelium. *Experimental eye research* 81, 629-638.
- Kafarnik, C., McClellan, A., Dziasko, M., Daniels, J.T., Guest, D.J., 2020. Canine corneal stromal cells have multipotent mesenchymal stromal cell properties in vitro. *Stem cells and development* 29, 425-439.
- Kalpravidh, M., Tuntivanich, P., Vongsakul, S., Sirivaidyapong, S., 2009. Canine amniotic membrane transplantation for corneal reconstruction after the excision of dermoids in dogs. *Veterinary research communications* 33, 1003.

- Kao, W.W., Thomas, V.J.C., 2016. Cell therapy of corneal diseases. *Cornea* 35, S9.
- Karageorgiou, V., Kaplan, D., 2005. Porosity of 3D biomaterial scaffolds and osteogenesis. *Biomaterials* 26, 5474-5491.
- Karamichos, D., Funderburgh, M.L., Hutcheon, A.E., Zieske, J.D., Du, Y., Wu, J., Funderburgh, J.L., 2014. A role for topographic cues in the organization of collagenous matrix by corneal fibroblasts and stem cells. *PloS one* 9, e86260.
- Katagiri, Y., Brew, S.A., Ingham, K.C., 2003. All six modules of the gelatin-binding domain of fibronectin are required for full affinity. *Journal of Biological Chemistry* 278, 11897-11902.
- Keivyon, K.R., Tseng, S.C., 1989. Limbal autograft transplantation for ocular surface disorders. *Ophthalmology* 96, 709-723.
- Kim, B.-S., Mooney, D.J., 1998. Development of biocompatible synthetic extracellular matrices for tissue engineering. *Trends in biotechnology* 16, 224-230.
- Koizumi, N., Cooper, L.J., Fullwood, N.J., Nakamura, T., Inoki, K., Tsuzuki, M., Kinoshita, S., 2002. An evaluation of cultivated corneal limbal epithelial cells, using cell-suspension culture. *Investigative ophthalmology & visual science* 43, 2114-2121.
- Kondo, M., Tamaoki, J., Sakai, A., Kameyama, S., Kanoh, S., Konno, K., 1997. Increased oxidative metabolism in cow tracheal epithelial cells cultured at air-liquid interface. *American journal of respiratory cell and molecular biology* 16, 62-68.
- Kovšca Janjatović, A., Mršić, G., Pirkić, B., Kiš, I., Capak, D., Gredelj Šimec, N., Kezić, D., Špoljarić, D., Crnjac, J., Popović, M., 2015. Subconjunctival application of allogenic limbal cells in dogs with corneal disorders. *Veterinarski arhiv* 85, 547-561.
- Ksander, B.R., Kolovou, P.E., Wilson, B.J., Saab, K.R., Guo, Q., Ma, J., McGuire, S.P., Gregory, M.S., Vincent, W.J., Perez, V.L., 2014. ABCB5 is a limbal stem cell gene required for corneal development and repair. *Nature* 511, 353.
- Kuijpers, A.J., Engbers, G.H., Krijgsveld, J., Zaat, S.A., Dankert, J., Feijen, J., 2000. Cross-linking and characterisation of gelatin matrices for biomedical applications. *Journal of Biomaterials Science, Polymer Edition* 11, 225-243.
- Kundu, S., 2014. *Silk biomaterials for tissue engineering and regenerative medicine*. Elsevier.

- Kundu, S., Kundu, B., Talukdar, S., Bano, S., Nayak, S., Kundu, J., Mandal, B.B., Bhardwaj, N., Botlagunta, M., Dash, B.C., 2012. Nonmulberry silk biopolymers. *Biopolymers* 97, 455-467.
- Lai, J.-Y., 2013. Corneal stromal cell growth on gelatin/chondroitin sulfate scaffolds modified at different NHS/EDC molar ratios. *International journal of molecular sciences* 14, 2036-2055.
- Lai, J.-Y., Chen, K.-H., Hsiue, G.-H., 2007. Tissue-engineered human corneal endothelial cell sheet transplantation in a rabbit model using functional biomaterials. *Transplantation* 84, 1222-1232.
- Lai, J.-Y., Ma, D.H.-K., 2017. Ocular biocompatibility of gelatin microcarriers functionalized with oxidized hyaluronic acid. *Materials Science and Engineering: C* 72, 150-159.
- Langer R, V.J., 1993. Tissue engineering. *Science* 260, 920-926.
- Lavker, R.M., Sun, T.-T., 2000. Epidermal stem cells: properties, markers, and location. *Proceedings of the national academy of sciences* 97, 13473-13475.
- Lawrence, B.D., Marchant, J.K., Pindrus, M.A., Omenetto, F.G., Kaplan, D.L., 2009. Silk film biomaterials for cornea tissue engineering. *Biomaterials* 30, 1299-1308.
- Lawrence, B.D., Omenetto, F., Chui, K., Kaplan, D.L., 2008. Processing methods to control silk fibroin film biomaterial features. *Journal of materials science* 43, 6967-6985.
- Leong, K., Cheah, C., Chua, C., 2003. Solid freeform fabrication of three-dimensional scaffolds for engineering replacement tissues and organs. *Biomaterials* 24, 2363-2378.
- Li, M., Ogiso, M., Minoura, N., 2003. Enzymatic degradation behavior of porous silk fibroin sheets. *Biomaterials* 24, 357-365.
- Lim, P., Fuchsluger, T.A., Jurkunas, U.V., 2009. Limbal stem cell deficiency and corneal neovascularization, In: *Seminars in ophthalmology*, pp. 139-148.
- Liu, J., Lawrence, B.D., Liu, A., Schwab, I.R., Oliveira, L.A., Rosenblatt, M.I., 2012. Silk fibroin as a biomaterial substrate for corneal epithelial cell sheet generation. *Investigative ophthalmology & visual science* 53, 4130-4138.
- Liu, M., Hu, P., Ding, K., 2011. The effect of serum concentration on the growth, proliferation and collagen secretion in mouse L929 fibroblasts. *Xi bao yu fen zi mian yi xue za zhi= Chinese journal of cellular and molecular immunology* 27, 736-739.

- Liu, Z., Huang, A.J., Pflugfelder, S.C., 1999. Evaluation of corneal thickness and topography in normal eyes using the Orbscan corneal topography system. *British journal of ophthalmology* 83, 774-778.
- Ljubimov, A.V., Saghizadeh, M., 2015. Progress in corneal wound healing. *Progress in retinal and eye research* 49, 17-45.
- Lu, Q., Hu, X., Wang, X., Kluge, J.A., Lu, S., Cebe, P., Kaplan, D.L., 2010. Water-insoluble silk films with silk I structure. *Acta biomaterialia* 6, 1380-1387.
- Ma, P.X., 2004. Scaffolds for tissue fabrication. *Materials today* 7, 30-40.
- Madden, P.W., Lai, J.N., George, K.A., Giovenco, T., Harkin, D.G., Chirila, T.V., 2011. Human corneal endothelial cell growth on a silk fibroin membrane. *Biomaterials* 32, 4076-4084.
- Maggs, D.J., Miller, P., Ofri, R., 2012. *Slatter's fundamentals of veterinary ophthalmology*. Elsevier Health Sciences.
- Maharajan, V.S., Shanmuganathan, V., Currie, A., Hopkinson, A., Powell-Richards, A., Dua, H.S., 2007. Amniotic membrane transplantation for ocular surface reconstruction: indications and outcomes. *Clinical & experimental ophthalmology* 35, 140-147.
- Marshall, G.E., Konstas, A.G., Lee, W.R., 1991. Immunogold fine structural localization of extracellular matrix components in aged human cornea II. Collagen types V and VI. *Graefe's archive for clinical and experimental ophthalmology* 229, 164-171.
- McClatchey, A.I., Yap, A.S., 2012. Contact inhibition (of proliferation) redux. *Current opinion in cell biology* 24, 685-694.
- Meek, K., Fullwood, N.J., 2001. Corneal and scleral collagens—a microscopist's perspective. *Micron* 32, 261-272.
- Meek, K.M., Boote, C., 2004. The organization of collagen in the corneal stroma. *Experimental eye research* 78, 503-512.
- Mei, H., Nakatsu, M.N., Baclagon, E.R., Deng, S.X., 2014. Frizzled 7 maintains the undifferentiated state of human limbal stem/progenitor cells. *Stem cells* 32, 938-945.
- Merindano, M.D., Costa, J., Canals, M., Potau, J., Ruano, D., 2003. A comparative study of Bowman's layer in some mammals: relationships with other constituent corneal structures. *European Journal of anatomy* 6, 133-140.

Meyer-Blazejewska, E.A., Kruse, F.E., Bitterer, K., Meyer, C., Hofmann-Rummelt, C., Wünsch, P.H., Schlötzer-Schrehardt, U., 2010. Preservation of the limbal stem cell phenotype by appropriate culture techniques. *Investigative ophthalmology & visual science* 51, 765-774.

Mikhailova, A., Jylhä, A., Rieck, J., Nättinen, J., Ilmarinen, T., Veréb, Z., Aapola, U., Beuerman, R., Petrovski, G., Uusitalo, H., 2015. Comparative proteomics reveals human pluripotent stem cell-derived limbal epithelial stem cells are similar to native ocular surface epithelial cells. *Scientific reports* 5, 14684.

Mimura, T., Tabata, Y., Amano, S., 2011. Transplantation of corneal stroma reconstructed with gelatin and multipotent precursor cells from corneal stroma, In: *Tissue Engineering for Tissue and Organ Regeneration*. IntechOpen.

Mittal, S.K., Omoto, M., Amouzegar, A., Sahu, A., Rezazadeh, A., Katikireddy, K.R., Shah, D.I., Sahu, S.K., Chauhan, S.K., 2016. Restoration of corneal transparency by mesenchymal stem cells. *Stem cell reports* 7, 583-590.

Moisenovich, M., Arkhipova, A.Y., Orlova, A., Volkova, S., Zacharov, S., Agapov, I., Kirpichnikov, M., 2014. Composite scaffolds containing silk fibroin, gelatin, and hydroxyapatite for bone tissue regeneration and 3D cell culturing. *Acta Naturae (англоязычная версия)* 6.

Morita, M., Fujita, N., Takahashi, A., Nam, E.R., Yui, S., Chung, C.S., Kawahara, N., Lin, H.Y., Tsuzuki, K., Nakagawa, T., 2015. Evaluation of ABCG 2 and p63 expression in canine cornea and cultivated corneal epithelial cells. *Veterinary ophthalmology* 18, 59-68.

Motta, A., Fambri, L., Migliaresi, C., 2002. Regenerated silk fibroin films: thermal and dynamic mechanical analysis. *Macromolecular Chemistry and Physics* 203, 1658-1665.

Nakatsu, M.N., González, S., Mei, H., Deng, S.X., 2014. Human limbal mesenchymal cells support the growth of human corneal epithelial stem/progenitor cells. *Investigative ophthalmology & visual science* 55, 6953-6959.

Nam, E., Fujita, N., Morita, M., Tsuzuki, K., Lin, H.Y., Chung, C.S., Nakagawa, T., Nishimura, R., 2015. Comparison of the canine corneal epithelial cell sheets cultivated from limbal stem cells on canine amniotic membrane, atelocollagen gel, and temperature-responsive culture dish. *Veterinary ophthalmology* 18, 317-325.

- Nickerson, J.F.H.J., 2015. *Molecular Biology of Eye Disease*, Academic Press.
- Nieto-Miguel, T., Calonge, M., de la Mata, A., López-Paniagua, M., Galindo, S., de la Paz, M.F., Corrales, R.M., 2011. A comparison of stem cell-related gene expression in the progenitor-rich limbal epithelium and the differentiating central corneal epithelium. *Molecular vision* 17, 2102.
- Nishi, C., Nakajima, N., Ikada, Y., 1995. In vitro evaluation of cytotoxicity of diepoxy compounds used for biomaterial modification. *Journal of biomedical materials research* 29, 829-834.
- Niu, G., Choi, J.-S., Wang, Z., Skardal, A., Giegegack, M., Soker, S., 2014. Heparin-modified gelatin scaffolds for human corneal endothelial cell transplantation. *Biomaterials* 35, 4005-4014.
- Numata, K., Cebe, P., Kaplan, D.L., 2010. Mechanism of enzymatic degradation of beta-sheet crystals. *Biomaterials* 31, 2926-2933.
- O'Brien, F.J., Harley, B.A., Yannas, I.V., Gibson, L.J., 2005. The effect of pore size on cell adhesion in collagen-GAG scaffolds. *Biomaterials* 26, 433-441.
- O'Neill, D.G., Lee, M.M., Brodbelt, D.C., Church, D.B., Sanchez, R.F., 2017. Corneal ulcerative disease in dogs under primary veterinary care in England: epidemiology and clinical management. *Canine genetics and epidemiology* 4, 5.
- Oliva, M.S., Schottman, T., Gulati, M., 2012. Turning the tide of corneal blindness. *Indian journal of ophthalmology* 60, 423.
- Ollivier, F.J., 2008. Use of equine amniotic membrane in ophthalmic surgeries in veterinary medicine. Google Patents.
- Omenetto, F.G., Kaplan, D.L., 2010. New opportunities for an ancient material. *Science* 329, 528-531.
- Osei-Bempong, C., Figueiredo, F.C., Lako, M., 2013. The limbal epithelium of the eye—a review of limbal stem cell biology, disease and treatment. *Bioessays* 35, 211-219.
- P De Miguel, M., Fuentes-Julian, S., Blazquez-Martinez, A., Y Pascual, C., A Aller, M., Arias, J., Arnalich-Montiel, F., 2012. Immunosuppressive properties of mesenchymal stem cells: advances and applications. *Current molecular medicine* 12, 574-591.
- Pahuja, P., Arora, S., Pawar, P., 2012. Ocular drug delivery system: a reference to natural polymers. *Expert Opinion on Drug Delivery* 9, 837-861.



- Park, S.H., Kim, K.W., Chun, Y.S., Kim, J.C., 2012. Human mesenchymal stem cells differentiate into keratocyte-like cells in keratocyte-conditioned medium. *Experimental eye research* 101, 16-26.
- Pellegrini, G., Golisano, O., Paterna, P., Lambiase, A., Bonini, S., Rama, P., De Luca, M., 1999. Location and clonal analysis of stem cells and their differentiated progeny in the human ocular surface. *The Journal of cell biology* 145, 769-782.
- Petrick, S., 1996. The incidence of eye disease in dogs in a veterinary academic hospital: 1772 cases. *Journal of the South African Veterinary Association* 67, 108-110.
- Philp, D., Chen, S.S., Fitzgerald, W., Orenstein, J., Margolis, L., Kleinman, H.K., 2005. Complex extracellular matrices promote tissue-specific stem cell differentiation. *Stem cells* 23, 288-296.
- Prakashan, N., 2005. *Pharmaceutical Microbiology Principles and Applications*. Tubitak.
- Prasertsung, I., Damrongsakkul, S., Saito, N., 2013. Crosslinking of a gelatin solutions induced by pulsed electrical discharges in solutions. *Plasma Processes and Polymers* 10, 792-797.
- Ratanavaraporn, J., Rangkupan, R., Jeeratawatchai, H., Kanokpanont, S., Damrongsakkul, S., 2010. Influences of physical and chemical crosslinking techniques on electrospun type A and B gelatin fiber mats. *International journal of biological macromolecules* 47, 431-438.
- Robert, L., Legeais, J., Robert, A., Renard, G., 2001. Corneal collagens. *Pathologie Biologie* 49, 353-363.
- Rockwood, D.N., Preda, R.C., Yücel, T., Wang, X., Lovett, M.L., Kaplan, D.L., 2011. Materials fabrication from Bombyx mori silk fibroin. *Nature protocols* 6, 1612.
- Ruiz-Ederra, J., Verkman, A., 2009. Aquaporin-1-facilitated keratocyte migration in cell culture and in vivo corneal wound healing models. *Experimental eye research* 89, 159-165.
- Sangwan, V.S., Basu, S., MacNeil, S., Balasubramanian, D., 2012. Simple limbal epithelial transplantation (SLET): a novel surgical technique for the treatment of unilateral limbal stem cell deficiency. *British Journal of Ophthalmology* 96, 931-934.
- Schlötzer-Schrehardt, U., Kruse, F.E., 2005. Identification and characterization of limbal stem cells. *Experimental eye research* 81, 247-264.

- Secker, G., Daniels, J., 2009. StemBook. Limbal epithelial stem cells of the cornea. The Stem Cell Research Community, StemBook.
- Sisson, K., Zhang, C., Farach-Carson, M.C., Chase, D.B., Rabolt, J.F., 2009. Evaluation of cross-linking methods for electrospun gelatin on cell growth and viability. *Biomacromolecules* 10, 1675-1680.
- Suzuki, S., Dawson, R.A., Chirila, T.V., Shadforth, A., Hogerheyde, T.A., Edwards, G.A., Harkin, D.G., 2015. Treatment of silk fibroin with poly (ethylene glycol) for the enhancement of corneal epithelial cell growth. *Journal of functional biomaterials* 6, 345-366.
- Talebian, A., Kordestani, S., Rashidi, A., Dadashian, F., Montazer, M., 2007. The effect of glutaraldehyde on the properties of gelatin films. *Kemija u industriji: Časopis kemičara i kemijskih inženjera Hrvatske* 56, 537-541.
- Tan, D.T., Ficker, L.A., Buckley, R.J., 1996. Limbal transplantation. *Ophthalmology* 103, 29-36.
- Taylor, Z.D., Garritano, J., Sung, S., Bajwa, N., Bennett, D.B., Nowroozi, B., Tewari, P., Sayre, J., Hubschman, J.-P., Deng, S., 2015. THz and mm-wave sensing of corneal tissue water content: electromagnetic modeling and analysis. *IEEE transactions on terahertz science and technology* 5, 170-183.
- Tighe, A., Williams, D., Analysis of lymphocyte populations in nictitans glands of dogs with keratoconjunctivitis sicca. *Veterinary Journal* submitted.
- Toricelli, A.A., Singh, V., Santhiago, M.R., Wilson, S.E., 2013. The corneal epithelial basement membrane: structure, function, and disease. *Investigative ophthalmology & visual science* 54, 6390-6400.
- Tsai, R., Tseng, S., 1994. Human allograft limbal transplantation for corneal surface reconstruction. *Cornea* 13, 389-400.
- Tseng, S.C., Prabhasawat, P., Barton, K., Gray, T., Meller, D., 1998. Amniotic membrane transplantation with or without limbal allografts for corneal surface reconstruction in patients with limbal stem cell deficiency. *Archives of Ophthalmology* 116, 431-441.
- Tungtasana, H., Shuangshoti, S., Shuangshoti, S., Kanokpanont, S., Kaplan, D.L., Bunaprasert, T., Damrongsakkul, S., 2010. Tissue response and biodegradation of

composite scaffolds prepared from Thai silk fibroin, gelatin and hydroxyapatite. *Journal of Materials Science: Materials in Medicine* 21, 3151-3162.

Utheim, O., Islam, R., Lyberg, T., Roald, B., Eidet, J.R., de la Paz, M.F., Dartt, D.A., Raeder, S., Utheim, T.P., 2015. Serum-free and xenobiotic-free preservation of cultured human limbal epithelial cells. *PLoS One* 10, e0118517.

Vongsakul, S., Tuntivanich, P., Sirivaidyapong, S., Kalpravidh, M., 2009. Canine amniotic membrane transplantation for ocular surface reconstruction of created deep corneal ulcers in dogs. *The Thai Journal of Veterinary Medicine* 39, 135-144.

Wang, L., Ma, R., Du, G., Guo, H., Huang, Y., 2015. Biocompatibility of helicoidal multilamellar arginine–glycine–aspartic acid-functionalized silk biomaterials in a rabbit corneal model. *Journal of Biomedical Materials Research Part B: Applied Biomaterials* 103, 204-211.

Wang, Y., Rudym, D.D., Walsh, A., Abrahamsen, L., Kim, H.-J., Kim, H.S., Kirker-Head, C., Kaplan, D.L., 2008. In vivo degradation of three-dimensional silk fibroin scaffolds. *Biomaterials* 29, 3415-3428.

Watanabe, R., Hayashi, R., Kimura, Y., Tanaka, Y., Kageyama, T., Hara, S., Tabata, Y., Nishida, K., 2011. A novel gelatin hydrogel carrier sheet for corneal endothelial transplantation. *Tissue engineering Part A* 17, 2213-2219.

Whitcher, J.P., Srinivasan, M., Upadhyay, M.P., 2001. Corneal blindness: a global perspective. *Bulletin of the world health organization* 79, 214-221.

Wiley, L., SundarRaj, N., Sun, T., Thoft, R., 1991. Regional heterogeneity in human corneal and limbal epithelia: an immunohistochemical evaluation. *Investigative ophthalmology & visual science* 32, 594-602.

Wilson, S.E., Mohan, R.R., Mohan, R.R., Ambrósio Jr, R., Hong, J., Lee, J., 2001. The corneal wound healing response:: cytokine-mediated interaction of the epithelium, stroma, and inflammatory cells. *Progress in retinal and eye research* 20, 625-637.

Wilson, S.L., Wimpenny, I., Ahearne, M., Rauz, S., El Haj, A.J., Yang, Y., 2012. Chemical and topographical effects on cell differentiation and matrix elasticity in a corneal stromal layer model. *Advanced Functional Materials* 22, 3641-3649.

- Wu, J., Du, Y., Mann, M.M., Funderburgh, J.L., Wagner, W.R., 2014a. Corneal stromal stem cells versus corneal fibroblasts in generating structurally appropriate corneal stromal tissue. *Experimental eye research* 120, 71-81.
- Wu, J., Du, Y., Mann, M.M., Yang, E., Funderburgh, J.L., Wagner, W.R., 2013. Bioengineering organized, multilamellar human corneal stromal tissue by growth factor supplementation on highly aligned synthetic substrates. *Tissue Engineering Part A* 19, 2063-2075.
- Wu, J., Du, Y., Watkins, S.C., Funderburgh, J.L., Wagner, W.R., 2012. The engineering of organized human corneal tissue through the spatial guidance of corneal stromal stem cells. *Biomaterials* 33, 1343-1352.
- Wu, J., Rnjak-Kovacina, J., Du, Y., Funderburgh, M.L., Kaplan, D.L., Funderburgh, J.L., 2014b. Corneal stromal bioequivalents secreted on patterned silk substrates. *Biomaterials* 35, 3744-3755.
- Wu, Z., Zhou, Q., Duan, H., Wang, X., Xiao, J., Duan, H., Li, N., Li, C., Wan, P., Liu, Y., 2014c. Reconstruction of auto-tissue-engineered lamellar cornea by dynamic culture for transplantation: a rabbit model. *PLoS One* 9, e93012.
- Yan, J., Qiang, L., Gao, Y., Cui, X., Zhou, H., Zhong, S., Wang, Q., Wang, H., 2012. Effect of fiber alignment in electrospun scaffolds on keratocytes and corneal epithelial cells behavior. *Journal of Biomedical Materials Research Part A* 100, 527-535.
- Yang, Z., Xu, L.S., Yin, F., Shi, Y.Q., Han, Y., Zhang, L., Jin, H.F., Nie, Y.Z., Wang, J.B., Hao, X., 2012. In vitro and in vivo characterization of silk fibroin/gelatin composite scaffolds for liver tissue engineering. *Journal of digestive diseases* 13, 168-178.
- Yeh, J., Tucker, N., 2005. The use of tisseel in oculoplastics. *Investigative Ophthalmology & Visual Science* 46, 4252-4252.
- Yu, W.Y., Sheridan, C., Grierson, I., Mason, S., Kearns, V., Lo, A.C.Y., Wong, D., 2011. Progenitors for the corneal endothelium and trabecular meshwork: a potential source for personalized stem cell therapy in corneal endothelial diseases and glaucoma. *BioMed Research International* 2011.
- Yung, C., Wu, L., Tullman, J., Payne, G., Bentley, W., Barbari, T., 2007. Transglutaminase crosslinked gelatin as a tissue engineering scaffold. *Journal of Biomedical Materials Research Part A: An Official Journal of The Society for Biomaterials, The Japanese*

Society for Biomaterials, and The Australian Society for Biomaterials and the Korean Society for Biomaterials 83, 1039-1046.

Zhu, X., Beuerman, R.W., Chan-Park, M., Cheng, Z., Ang, L.P., Tan, D.T., 2006. Enhancement of the mechanical and biological properties of a biomembrane for tissue engineering the ocular surface. ANNALS-ACADEMY OF MEDICINE SINGAPORE 35, 210.

Zieske, J.D., Mason, V.S., Wasson, M.E., Meunier, S.F., Nolte, C.J., Fukai, N., Olsen, B.R., Parenteau, N.L., 1994. Basement membrane assembly and differentiation of cultured corneal cells: importance of culture environment and endothelial cell interaction. Experimental cell research 214, 621-633.



## VITA

**NAME** Chutirat Torsahakul

**DATE OF BIRTH** 24 Sep 1985

**PLACE OF BIRTH** Bangkok

**INSTITUTIONS ATTENDED** Chulalongkorn University

**HOME ADDRESS** 3761/431 Soi Yudi 5 Bangklo Bangkholaem Bangkok 10120

**AWARD RECEIVED** Ph.D. Scholar in “The 100th Anniversary Chulalongkorn University for Doctoral Scholarship”, Graduate school, Chulalongkorn university, Thailand (since academic year 2016)

